

Final Report:
**CONTROLLED ELEVATOR SAFETY
MECHANISM**

ME450, Winter 2008
Section 3, Team 8

Members:

James Moss
Michael Rayle
Marco Shek
Tong Zhang

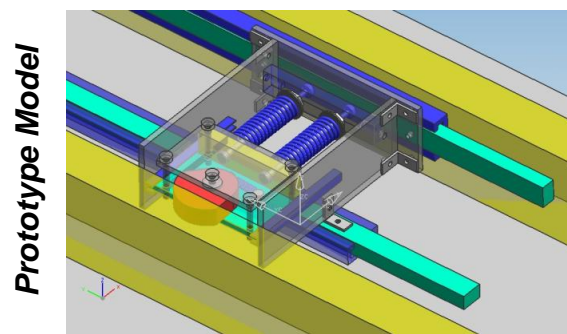
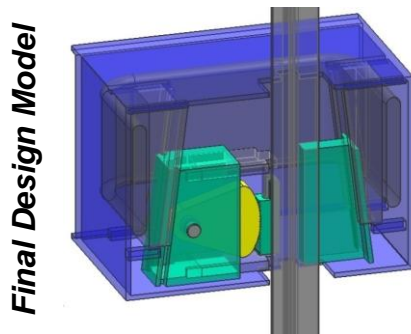
Section Instructor:
Prof. Gregory Hulbert

April 15, 2008

EXECUTIVE SUMMARY

DESIGN PROBLEM Existing elevator safety mechanisms are susceptible to variable friction conditions, which cause an inconsistent deceleration during emergency stops. The braking mechanism provides a constant normal force, which means the braking force and subsequent deceleration are proportional to the varying coefficient of friction (μ) between the brakes and the rail. Our goal is to design and manufacture a proof-of-concept prototype for a mechanically self-adjusting safety that produces a constant deceleration (0.6 ± 0.05 g) in spite of variable friction conditions ($0.15 < \mu < 0.25$) during emergency stops.

FINAL DESIGN The selected final design uses a rotating cam that acts as a friction sensor and as a brake. A vertical spring is attached to the cam and it provides a moment to help maintain constant contact with the rail and to oppose the upward and horizontal forces from the rail. The cam is contained in a wedge-shaped frame similar to the wedge on the existing design and a U-spring produces a compressive normal force on the frame. As a result, when μ increases the cam rotates upward and its radius (pivot-to-rail) decreases, which decreases the normal force. The inverse relationship between μ and the normal force results in a constant braking force and constant deceleration. Rather than contacting the rail directly, the cam contacts a brake shoe via a set of teeth (à la a rack-and-pinion mechanism). The brake shoe allows for a larger braking surface to help dissipate heat and contact forces.



PROTOTYPE A proof-of-concept prototype was fabricated as physical validation for our design. The dimensions and forces are scaled down from the final values and the mechanism is simplified; however, the dynamic principles remain the same. Instead of falling along the vertical axis, the prototype is pulled along the horizontal axis by a force gauge to measure the tangential force.

PHYSICAL VALIDATION The prototype was tested on three different surfaces with μ equal to 0.20, 0.30, and 0.45. It is clear that for a greater μ , the cam rotates more and the normal force decreases, which agrees with our analysis. It was measured that a 50% increase in μ results in only a 10% increase in tangential force. Remaining variations in the tangential force can be attributed to non-ideal testing conditions, imprecise force measurements, and differences between the experimental and calculated spring constants.

VIRTUAL VALIDATION A virtual simulation has been created using ADAMS software. The simulation uses one safety block with two cams and the full-scale parameters. It demonstrates that, for a 40% change in μ , the acceleration changes by only 8%. For $0.15 < \mu < 0.25$, the deceleration remains equal to 0.6 ± 0.05 g. An animation has been generated that shows the rotation of the cam across different friction surfaces.

OUTCOMES & RECOMMENDATIONS Based on the results from the physical and virtual testing, the design concept appears feasible. The full-scale version will see much higher forces and special considerations must be made to dissipate the large amount of stress and heat. An extensive analysis should be conducted on the rack-and-pinion geometry and alternatives should be contemplated as well. Tests should be run with a full-scale prototype and several refinements will likely be necessary to reach an optimum design.

TABLE OF CONTENTS

1	Introduction	1
1.1	Problem Definition.....	1
1.2	Project Sponsor	2
1.3	Customer Requirements	2
2	Engineering Specifications	3
2.1	Engineering Parameters.....	3
2.2	QFD.....	3
3	Concept Generation.....	4
3.1	System Analysis.....	4
3.2	Brainstorming	5
3.3	Concept Classifications	5
3.3.1	Sensor types	6
3.3.2	Transmission types	6
3.3.3	Brake types	6
3.3.4	Non-Feedback Concepts	6
3.4	Concept Exploration.....	6
3.5	Top Designs	7
3.5.1	Rotating Cam	7
3.5.2	Screw in U-spring.....	8
3.5.3	Double Wedge.....	8
3.5.4	Mass-Spring-Lever	9
3.5.5	Multi-Wedge	9
4	Concept Selection Process.....	10
4.1	Concept Elimination.....	10
4.2	Selection Tools	10
4.2.1	QFD.....	10
4.2.2	Pugh Chart	10
5	Final Design Description.....	11
5.1	Concept Description.....	11
5.2	Overview of Mechanism	12
5.3	Final Design Parameter Analysis	12
5.3.1	Static Equilibrium Analysis	13
5.3.2	Pin Diameter of Final Design.....	13
5.3.3	Rack and Pinion Mechanism.....	14
5.4	Manufacturing Analyses.....	15
5.4.1	Material and Manufacturing Process Selection.....	15
5.4.2	Design for Assembly	16
5.4.3	Design for Environment.....	16
5.4.4	Design for Safety.....	16
6	Prototype Description.....	16
6.1	Design Simplifications	17
6.1.1	Horizontal Setup.....	17
6.1.2	Single cam.....	17
6.1.3	Pre-engagement.....	17
6.2	Scaled Parameters	17
6.2.1	Cam Profile Dimensions	17
6.2.2	Spring Constants & forces	18
6.2.3	Materials & Friction Coefficients.....	18
7	Fabrication Plan	18
7.1	Custom Parts.....	19

7.2	Standard Parts	19
7.3	Assembly Instructions	19
7.3.1	Cam Frame Sub-Assembly	20
7.3.2	Casing Sub-Assembly.....	20
7.3.3	Base Sub-Assembly.....	20
7.3.4	Main Assembly	20
7.4	Prototype Fabrication versus Final Design Manufacturing	21
8	Validation Plan	21
8.1	Physical Prototype Demonstration.....	21
8.1.1	Determination of Friction Coefficients	21
8.1.2	Prototype Test Results	22
8.2	Virtual Dynamic Simulation.....	23
9	Discussion	24
10	Future Work.....	25
11	Conclusions	25
12	Acknowledgements.....	26
13	Information Sources	26
13.1	Sponsor Information.....	26
13.2	Supplemental Materials.....	26
14	References	27
Appendix A	Current Safety Engineering Drawing	28
Appendix B	Supplemental Analyses.....	29
Appendix C	Final Design Dimensioned Drawings	31
Appendix D	Prototype Dimensioned Drawings.....	35
Appendix E	Engineering Change Notices.....	39
Appendix F	Bill of Materials	41
Appendix G	Prototype Process Sheets	42
Appendix H	Complete Test Results	44
Appendix I	Complete Gantt Chart.....	45
Appendix J	Brainstorming Concepts	46
Appendix K	Prototype Photographs.....	55
Appendix L	Design Analyses	56

1 INTRODUCTION

1.1 Problem Definition

Elevator safeties are devices attached to the bottom of an elevator car that are designed to bring the car to a safe stop in the event of uncontrolled runaway or freefall. This type of event can arise during critical control system failure or during a catastrophic event, such as all drive ropes being cut. Current elevator safeties (see Figure 1 for photograph, Appendix A for engineering drawing) are actuated when a speed-sensing governor mounted at the top of the elevator shaft detects an over-speed condition. The governor tugs on a set of safety ropes, which then forces a pair of wedges to rise and self-engage (see Figure 2) the elevator guide rail to stop the elevator car.

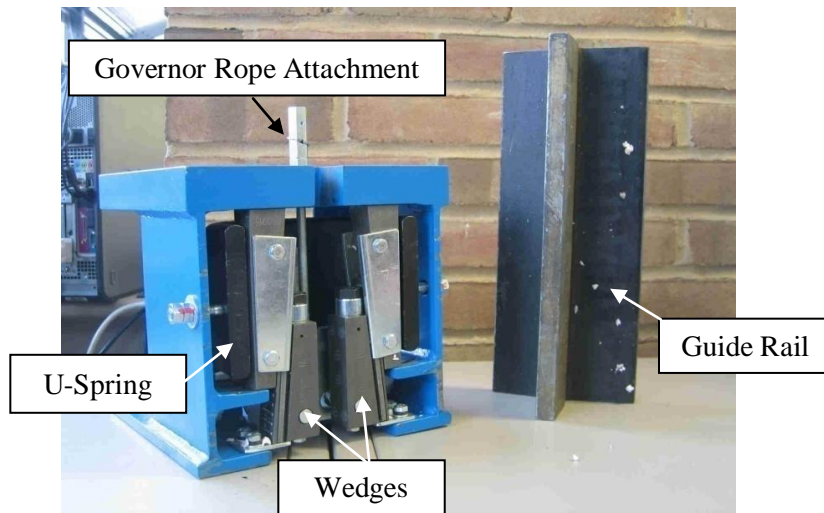


Figure 1. Current elevator safety

The braking force is determined by a preset U-spring that wraps around the wedges and provides a constant calibrated normal force. The overall braking force is susceptible to changing friction conditions that are present between the wedges and the rail. The coefficient of friction can depend on wear and cleanliness of the rail, heat, and other unpredictable variables. The erratic friction conditions lead to undesirable variations in deceleration from one braking event to another. For example, one event could have an average deceleration of 0.4 g and the next could have an average deceleration of 0.6 g.

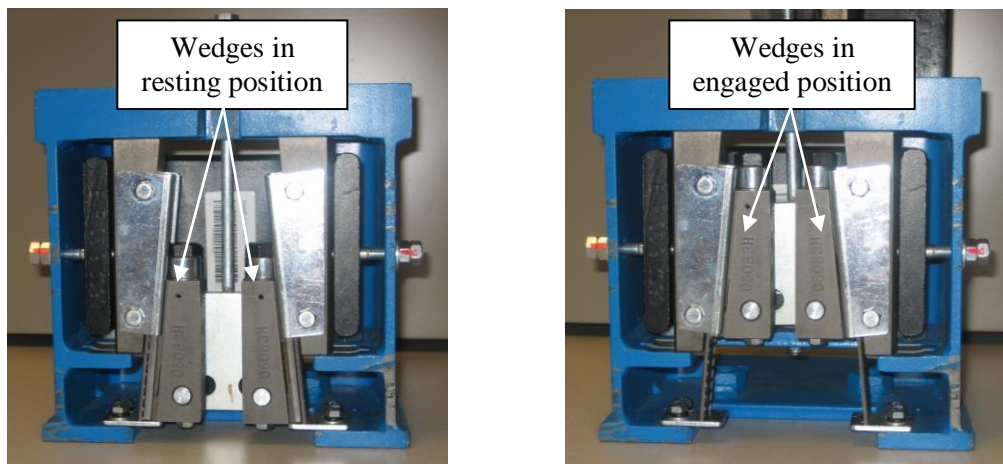


Figure 2. Photographs of safety in disengaged (left) and engaged (right) positions

Figure 3 shows the speed and deceleration of a car during one such dynamic stopping event, starting when the safety is engaged at 1.9 seconds and ending at 3.4 seconds when the car velocity is zero. Once the safety engages, the deceleration remains roughly constant at about 0.4 g until the final half-second, during which the deceleration ramps up to 3.0 g.

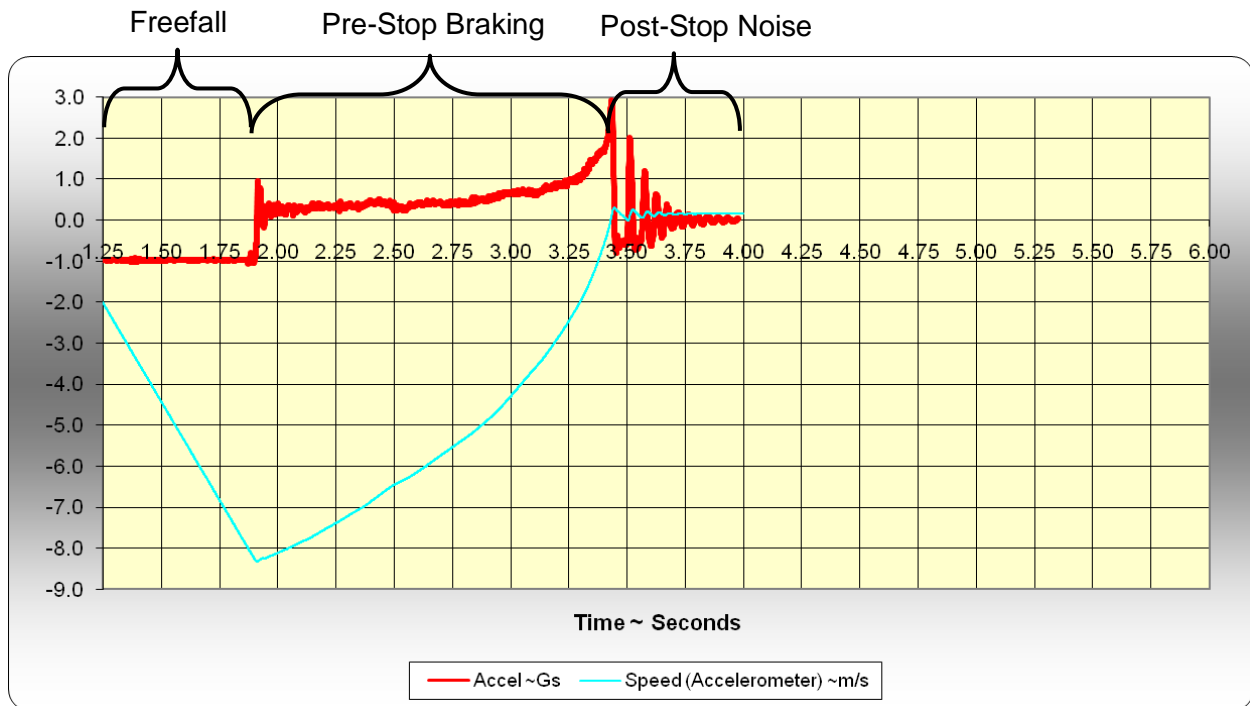


Figure 3. Drop test data with upper curve showing varying deceleration [7]

The design challenge is to explore mechanical alternatives that would compensate for the variation of friction from actuation to actuation as well as during a dynamic event. We intend to design and fabricate a proof-of-concept prototype for a self-adjusting, purely mechanical elevator safety that produces a constant deceleration in spite of variable friction conditions during emergency stops.

1.2 Project Sponsor

Our sponsor is the Otis Elevator Company located in Farmington, Connecticut. Our lead contact is Nigel Morris who is the head of Engineering Safety Components at Otis. Our group will also be working with Jim Draper whom will act as a mentor and technical advisor.

1.3 Customer Requirements

The main project requirements were defined by Otis to resolve issues with current safeties due to variable friction conditions. The overall objective of the alpha prototype is to produce a constant deceleration during an emergency stop. To achieve this, the design must self-adjust the applied normal force according to the variations of friction between brakes and rail.

Otis also placed the following constraints on the design concept:

- No external power sources shall be used to apply normal to the friction surface. (No hydraulics, pneumatics, or electro-magnets allowed). Permanent magnet technology may be considered.
- The device must be purely mechanical (springs, linkages, wedges, etc.).
- The device shall not limit vertical motion of the elevator when not in use.
- The operating range of dynamic coefficient of friction shall be 0.15 to 0.25.

- The device must be self-engaging once the friction surfaces touch the guide rails.
- The device must self disengage when the external tangential force is removed.
- The device cannot infringe on any existing patents for elevator devices.

In addition, the design should comply with the following requirements for current safeties:

- Low-cost (\$100-\$200)
- Long-lasting (25 actuations)
- Does not damage safety blocks or guide rails during actuation
- Easy to manufacture and assemble

Otis also added that it is highly beneficial to have the braking surface function also as the friction sensor because using a separate friction sensor would not guarantee that the two friction interfaces are equivalent.

2 ENGINEERING SPECIFICATIONS

At the beginning of the project, Otis provided specifications for the elevator system to help define the critical parameters. These values were then analyzed and a Quality Function Deployment (QFD) was developed to relate technical specifications to customer requirements.

2.1 Engineering Parameters

Otis has provided the following quantities in Table 1. The mass (m) of the elevator car is assumed to be constant, so the required braking force (F_T) is proportional to the deceleration (a) by Newton's Second Law, $F_T = ma$. The required normal force, F_N , to produce this braking force is found using the equation $F_N = F_T/\mu$. Hence, as the coefficient of friction increases, the normal force needs to decrease. The deceleration should remain constant at 0.6 ± 0.05 g over the range $0.1 < \mu < 0.4$. The lifetime, cost, and quantity are factors that will be considered for mass production.

Specified Parameters	Symbol	Value	Units
Elevator Car Mass	m	4500	kg
Coefficient of Friction	μ	0.15–0.25	--
Elevator Car Speed		2.5	m/s
Target Quantities			
Deceleration of Car	a	0.6 ± 0.05	g
Braking Force / Unit	F_T	35	kN
Lifetime / Unit		25	Actuations
Cost / Unit		100–200	\$
Quantity / Year		40,000	Units

Table 1. Sponsor-defined quantities

The coefficient range was originally defined as 0.1–0.4. However, Otis has since relaxed this requirement to only cover 0.15–0.25.

2.2 QFD

The QFD had been the same as that in DR#2 (see Table 2, p. 4). The top three ranks on technical requirements are complexity of wedge, number of parts, and response time. These factors were given the greatest consideration in the concept selection phase.

Weight (-)		9												
Outer Dimensions (-)		3	3											
Response Time (-)		3	3											
Cost of Material per Unit (-)		9	9			3								
Number of Parts (-)		3	3	3	3									
Complexity of Wedge (-)		3	3	3	3									
		Technical Requirements							Current Safety					
Customer Needs	Customer Weights		Weight (-)	Outer Dimensions (-)	Response Time (-)	Cost of Material per Unit (-)	Number of Parts (-)	Complexity of Wedge (-)						
									1 Poor	2	3 Acceptable	4	5 Excellent	
Affordable	4		3	3		9	9	3						A
Works with Standard Rails	5			3			1	1						A
Quick Response Feedback	4				9		3	3		A				
Filters out High Freq.	3						3			A				
Constant Deceleration	5		1		9			9			A			
Compact Size	2		3	9			9	1						A
Long Lifetime (25 stops)	3						3	3						A
Easy to Disengage	3						3	9						A
Lightweight	1		9	3			1							A
Easy to Manufacture	2			3	3		9	3						A
	Raw score		32	54	87	36	117	118						
	Scaled		0.27	0.46	0.74	0.31	0.99	1.00						
	Relative Weight		7%	12%	20%	8%	26%	27%						
	Rank		6	4	3	5	2	1						
Technical Requirement Units			kg	m	ms	Dollars	#	# of flat surfaces						
Technical Requirement Targets			20	0.3		100		6						
Technical Requirement USL			30	0.5		200		9						

Table 2. QFD diagram with relative rankings of technical parameters

3 CONCEPT GENERATION

Concept generation was the first step in the overall design process and required the most creativity. Our sponsor asked for novel ideas that could extend beyond the limitations of their current designs. To begin, we held a brainstorming session to generate as many ideas as possible. These concepts were grouped into categories and a functional decomposition was used to help evaluate each design.

3.1 System Analysis

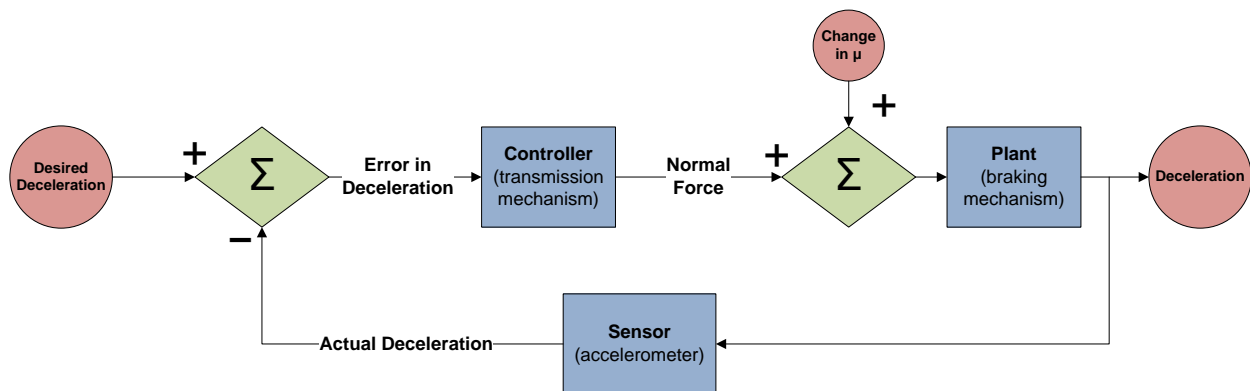


Figure 4. Self-adjusting safety analyzed as a feedback control system

As a basis for much of our concept generation, a feedback system (see Figure 4, p. 4) was considered as a means of creating a self-adjusting safety. The system operates by using a sensor to quantify the error in declaration (or tangential force or friction) and correspondingly adjusts the normal force. Other non-feedback designs were also considered.

3.2 Brainstorming

The brainstorming process generated a large number of rough ideas for solving the design problem. These solutions centered on creating a mechanism to sense the deceleration or coefficient of friction and a way to adjust and transmit this signal to the braking mechanism. The initial focus was on quantity rather than quality and personal judgment had to be suppressed. Only general engineering fundamentals, such as spring forces and friction forces, were considered at this point—actual calculations were reserved for the concept exploration phase.

At first, all ideas were new and most were based on modifying or enhancing the existing elevator safety design. Once a first wave of ideas was formed, these ideas were refined to improve feasibility and functionality. For example, the idea of using a cam as a friction sensor evolved from using the cam as an accelerometer with a translating center of mass.

3.3 Concept Classifications

Figure 5 illustrates the wide array of concepts that were considered. The feedback designs can be divided up into three categories: sensor type, transmission type, and brake type. The non-feedback designs attempt to solve the problem without self-adjustment.

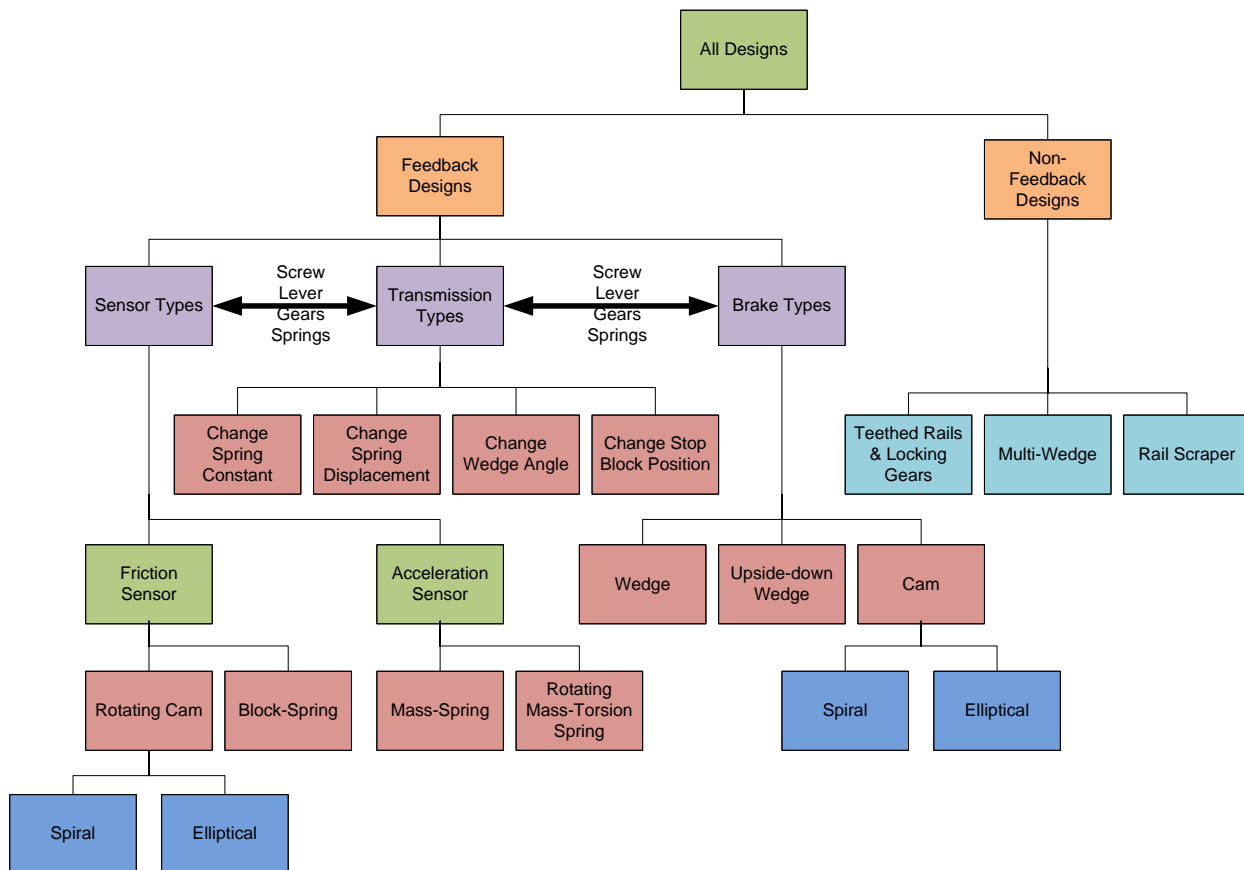


Figure 5. Concept classification tree showing how each concept can be broken down

3.3.1 Sensor types

The purpose of the sensor is to identify the current deceleration of the elevator car and to adjust the braking force accordingly. Two means of detecting the deceleration of the car both employ the displacement of a mass connected to a vertical spring. One design uses a mass with a linear spring, while the other uses an unbalanced mass that rotates and connects to a torsion spring. Whether the displacement is translational or rotational, this movement can be used to adjust the normal force on the brakes.

An alternative to the accelerometer method is to sense the coefficient of friction, μ , at the brake/rail interface. This can be done via a block that rubs against the rail. The block is connected to a spring parallel to the rail and the block displaces a distance proportional to μ . Similarly, a cam with increasing radius can be used along with a torsion spring to detect μ . Two possible shapes for the cam include a spiral (constantly increasing radius) and an ellipse.

3.3.2 Transmission types

The purpose of the transmission is to accept a signal from the sensor and use it to maintain a constant braking force and a constant deceleration. The most straightforward way to change the braking force is to change the normal force on the brakes, since μ is constant. One way to do this is to incorporate springs with pre-selected spring constants that will provide a known force per displacement. Other simple machines such as screws, gears, levers, and inclined planes were also considered to provide a mechanical advantage when trying to generate high braking forces.

3.3.3 Brake types

The actual shape of the braking shoes depends mostly on the type of sensor and transmission. A wedge is used in current safeties and is effective in converting kinetic energy into a large normal force. An upside-down wedge would not have this effect; however, it would automatically adjust the normal force based on μ in the desired manner. The cam design does not have as large a contact area, however, it can act as a sensor and brake and a torsion spring will maintain a large enough normal force to produce the desired deceleration.

3.3.4 Non-Feedback Concepts

The category of non-feedback mechanisms was ultimately discarded based on the lack of self-adjustment. However, they could work in certain controlled circumstances or they could be modified to incorporate feedback. See Appendix J for drawings and descriptions.

3.4 Concept Exploration

The main function of the proposed elevator safety is to self-adjust to generate a constant deceleration. This function was then broken down into many sub-functions in the form of a functional decomposition (see Figure 6, p. 7). The functional decomposition represents *what* has to be accomplished and the design process represents *how* to accomplish it.

The functional decomposition was used to ensure all sub-functions were addressed in the design phase. The design information that can be extracted from this diagram is contained mainly in the orange rectangular boxes, which are processes that require a mechanical form. The purple trapezoids represent inputs, be they forces or pre-calibrated information, while the red ovals represent outputs. The blue diamonds indicate mechanical governing equations and the green shapes signify quantities such as forces and accelerations that are transmitted between subsystems.

The Concept Exploration phase was also used as an opportunity to do preliminary analyses on some of the designs. Approximate forces and spring constants were derived to evaluate the feasibility of the concepts.

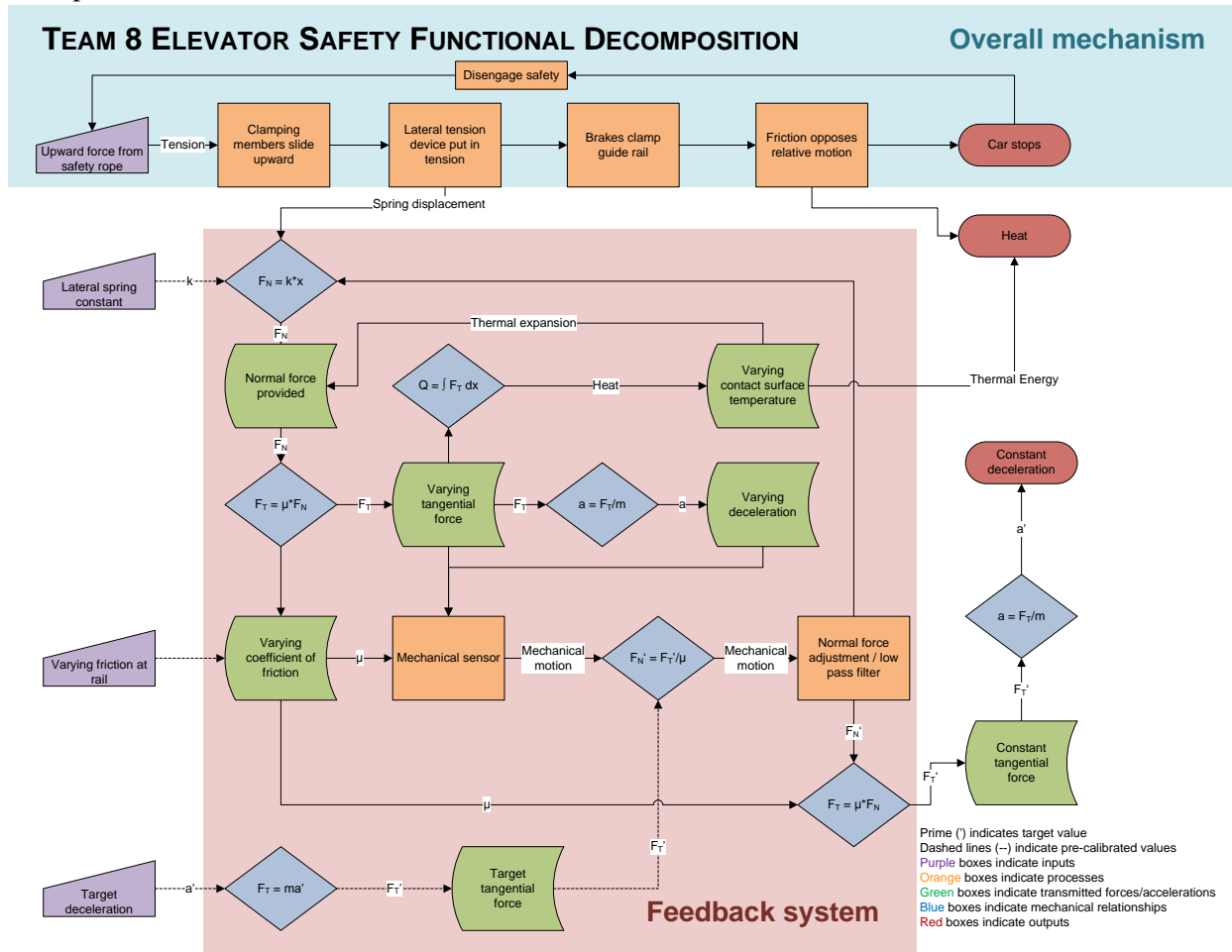


Figure 6. Functional decomposition

3.5 Top Designs

Our top five designs encompass all of the major concept classifications. They are full concepts that include sensor, transmission, and brake mechanisms (excluding the multi-wedge).

3.5.1 Rotating Cam

This design uses a rotating cam attached to a torsion spring (later replaced by a compression spring attached at an offset from the cam pivot) as a friction sensor and a braking surface (see Figure 7, p. 8). When μ increases, the cam rotates to a smaller radius (from U-spring to rail), thus decreasing the spring displacement and subsequent normal force. See Section 5 for a detailed description and analysis.

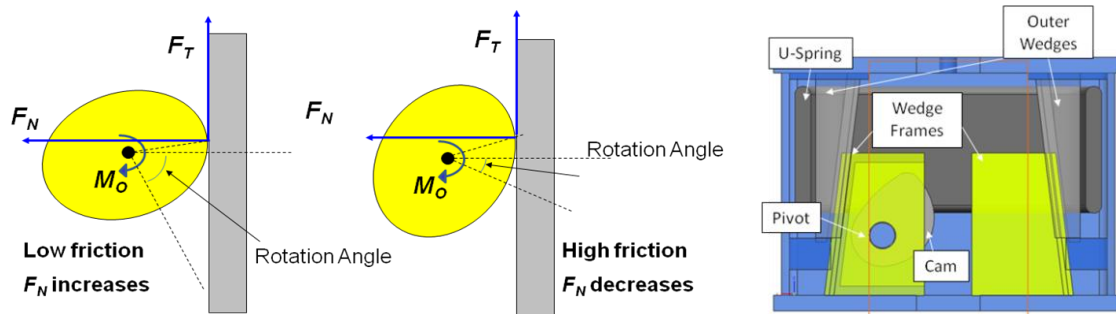


Figure 7. Rotating-cam concept (left) and drawing

3.5.2 Screw in U-spring

The screw in U-spring design (see Figure 8) utilizes a block as the friction sensor, with the same material properties as the braking wedges. It is attached to a spring in the vertical direction, the other end of which is attached to the safety block housing. There are also horizontal springs between the sensor block and the wedge to ensure a constant force normal to the rail surface. This force can be controlled by changing the horizontal springs.

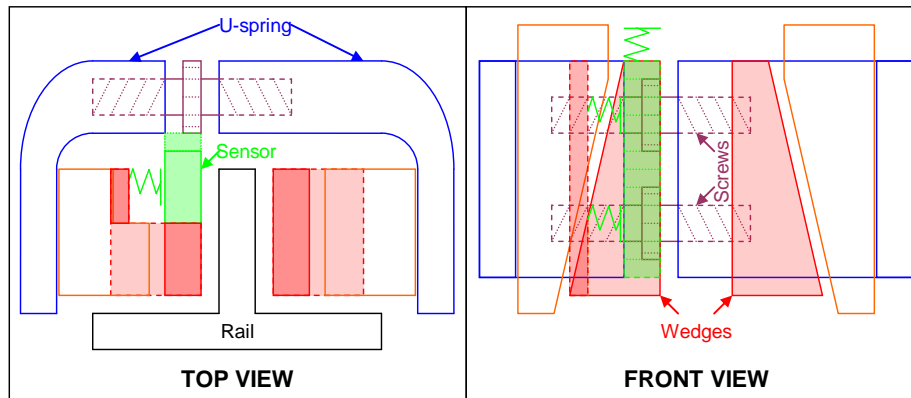


Figure 8. Screw in U-spring drawing

When the coefficient of friction between the wedges and rail increases, the sensor block moves upward. The back of the block has teeth that engage two gears, which in turn rotate two screws. These screws have opposite threading on either end and they loosen when the sensor block moves upward. The loosening of the screws releases tension on the U-spring and reduces the normal force on the wedges. This reduction in normal force compensates for the increase in friction and thus maintains a constant tangential force. A complete analysis is included in Appendix B.2.

3.5.3 Double Wedge

The double wedge design (see Figure 9, p. 9) consists of an inverted wedge inside of a conventional wedge. The outer conventional wedge is pulled up by the safety rope in the same sense as the current safety. After it is fully engaged, it locks into place and the inverted wedge is free to move up and down as a friction sensor. As the friction increases, the inner wedge moves upward and the U-spring displacement decreases, thus decreasing the normal force.

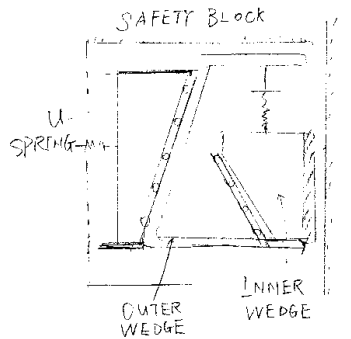


Figure 9. Double-Wedge Drawing

3.5.4 Mass-Spring-Lever

The mass-spring-lever design (see Figure 10) utilizes a mechanical accelerometer to detect the motion of the elevator car. A mass, which is free to translate along the vertical axis, is attached to a spring. When the elevator decelerates a given amount, the mass displaces proportionally in the downward direction. This displacement corresponds to a change in normal force via a lever system.

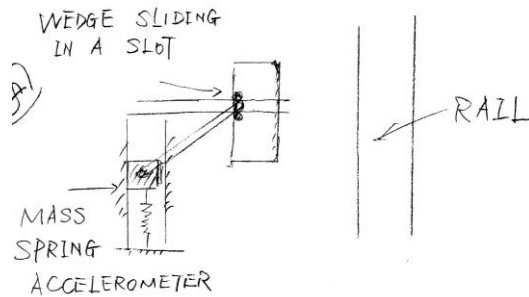


Figure 10. Mass-Spring-Lever drawing

3.5.5 Multi-Wedge

The multi-wedge design consists of multiple wedges that act to normalize the variation in friction. Although the original idea (see Figure 11) did not include a feedback system, one could be added to control the number of wedges that are engaged. When the friction decreases, more wedges would engage.

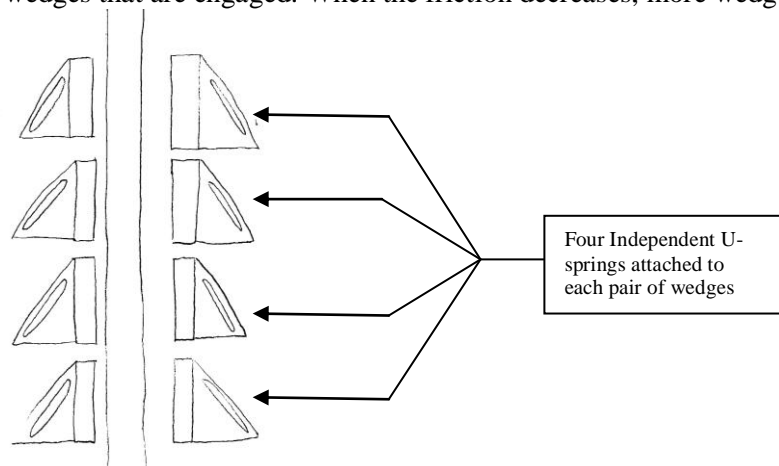


Figure 11. Multi-Wedge drawing

4 CONCEPT SELECTION PROCESS

The concept selection phase took place on many levels, from eliminating the infeasible designs to evaluating the feasible ones based on sub-functions. In the end, the rotating cam design was determined to be the best option because it satisfies all of the requirements while maintaining a desirable simplicity.

4.1 Concept Elimination

Several of our designs did not meet the customer requirements or exceeded size constraints. The multi-wedge and rail scraper designs could work depending on the nature of the varying friction. However, without a feedback system, these designs would not be universal enough to be used in certain environments. The teathed rail/locking gears design would work in any environment; however, it would require the installment of new, more expensive guide rails. Designs that did not include a feedback system were discarded in favor of the true feedback designs.

The concepts that utilized a mass-spring accelerometer were eliminated due to the unreasonable weight requirements. The sensor mass would have to be approximately the same as the mass of the elevator car in order to produce the required change in the normal force. Applying a mechanical advantage that would make the mass negligible would not produce the required spring displacement. The designs that remained used a friction sensor and a spring for the transmission.

The double wedge design seemed feasible; however, a patent was found with an almost identical design [12]. Furthermore, the design would require a complex mechanism to lock the outer wedge into place and it would require a counter-mechanism to reverse the process when the safety is reset.

The multi-wedge design could incorporate a feedback system to control which wedges are engaged. Springs could be used to engage more springs as the friction decreases. However, it would be difficult to reverse this process and disengage the springs when the friction increases.

4.2 Selection Tools

To evaluate the aforementioned mechanisms impartially, a systematic process was applied to each of the top concepts. The QFD rankings were used to identify the advantages and disadvantages of each design and a Pugh chart was formulated to assign each design a score based on how well it accomplishes the customer requirements.

4.2.1 QFD

The project QFD (see Table 2, p. 4) was used to assess the form of each design. Since the wedge profile and total number of parts had the largest impacts on the customer requirements, they were two of the top design considerations. The rotating cam design uses a curved profile to serve a dual purpose as brake and friction sensor, thus reducing the number of parts. This inherent characteristic is what made it the most attractive design. Other designs that included screws and gears would not be as robust or reliable.

4.2.2 Pugh Chart

A Pugh chart (see Table 3, p. 11) was utilized as the format for scoring each concept based on function. This method accounted for the strengths and weaknesses of each design on a weighted scale, with the existing safety as the zero reference. The weighting for the customer requirements is the same as those for the QFD diagram. Cost was removed as a customer requirement because it was too difficult to estimate at this point in the design process. Nevertheless, cost is inherent in the size and manufacturability of each design.

Criteria	Weight	Datum	Design 1	Design 2	Design 3	Design 4	Design 5
		Current Safety	Rotating Cam	Screw in U-spring	Double Wedge	Mass-Spring	Multi-Wedge
Works with Standard Rails	5	0	0	0	0	0	0
Quick Response Feedback	4	0	3	2	3	1	2
Constant Deceleration	5	0	3	2	3	1	1
Compact Size	2	0	-1	-3	-2	-3	-3
Long Lifetime	3	0	-2	-1	-2	-1	-2
Easy to Disengage	3	0	0	0	-3	0	-3
Lightweight	1	0	-1	-3	-2	-3	-3
Easy to Manufacture	2	0	-2	-1	-3	-2	-2
		Total	14	4	0	-7	-15

Table 3. Pugh chart with each of the top five designs weighted against the current design

The Pugh chart is not an end-all tool for concept selection; however, it does serve as a general ranking scheme. It is evident that the cam design is functionally more effective than the other designs, which agrees with our previous analysis and judgment.

5 FINAL DESIGN DESCRIPTION

The rotating cam with rack and pinion was selected as the final design. The next step was to analyze the different parameters of the design so the system could be modeled.

5.1 Concept Description

The selected concept is summarized in Figure 12. The safety uses a rotating cam (1) that acts as a friction sensor and as a brake. A restoring spring (2) is attached to the cam and it provides a moment to help maintain constant contact with the rail and to oppose the normal (3) and tangential (4) forces from the rail. The cam is contained in a frame (5) and a compression spring (6) produces a compressive force (7) on the frame. As a result, when μ increases the cam rotates upward and its radius (pivot-to-rail) decreases, which decreases the normal force. The inverse relationship between μ and the normal force results in a constant braking force ($F_T = \mu F_N$) and constant deceleration ($a = F_T/m$, $m = \text{constant}$).

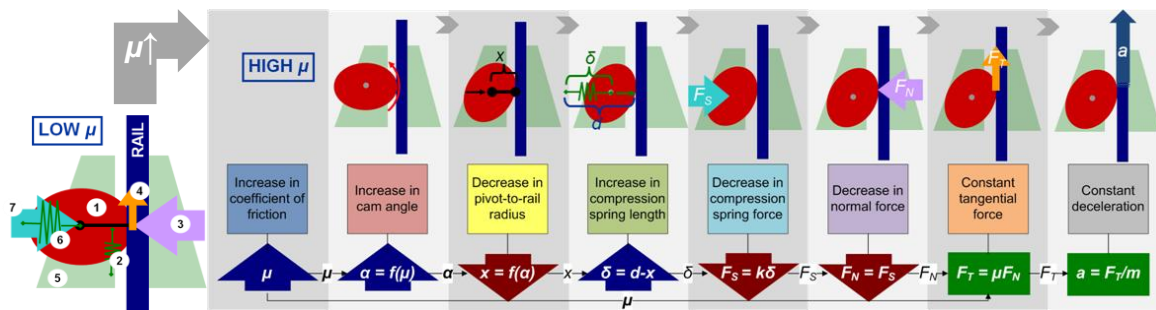


Figure 12. Selected concept diagram

5.2 Overview of Mechanism

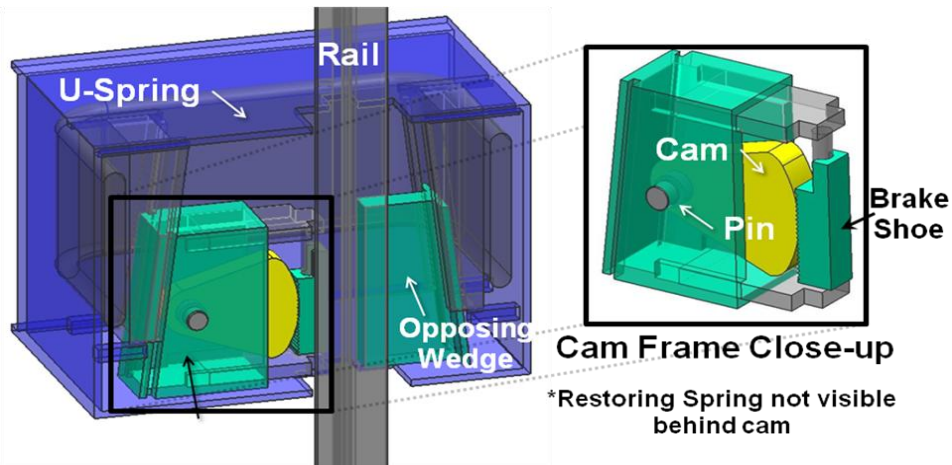


Figure 13. Isometric view of CAD model for rotating cam design with detail view of cam frame (right)

The final design works similar to the current safety design by incorporating a wedge design for engagement but it varies once engaged because one wedge represents a rotating cam subsystem. The cam subsystem comprises a cam and braking shoe acting as a rack and pinion, a pin joint, a restoring spring, and a frame (see Figure 13). The cam and frame subsystem replaces the wedge-shaped braking shoe in the standard safety design. The final design engages similar to the standard one: when the safety system is engaged by the governor ropes, the cam and its frame slide up and engage the rail, as shown in Figure 14. During the braking process, the cam can rotate about the pivot and will do so based on the amount of friction so as to provide constant deceleration. The preloaded restoring spring provides a force about a moment arm to counteract the moments exerted by the normal and tangential forces on the contact surface between the brake shoe and the rail. The frame will have pin restraints so that the cam's rotation is constrained to a certain range of friction coefficients.

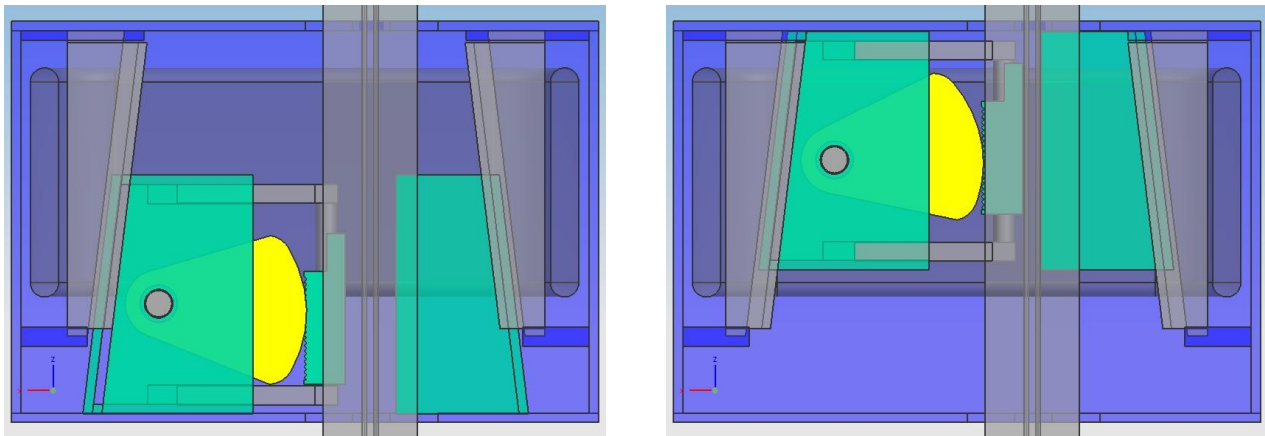


Figure 14. Rotating cam design in the disengaged position (left) and engaged position

5.3 Final Design Parameter Analysis

Once the rotating-cam design was chosen, calculations were done to optimize the braking performance for the specified range of friction coefficients ($0.15 < \mu < 0.25$) using a force balance analysis. Also, the geometry of the pin and rack-and-pinion mechanism had to be evaluated to ensure the structural reliability of the design.

5.3.1 Static Equilibrium Analysis

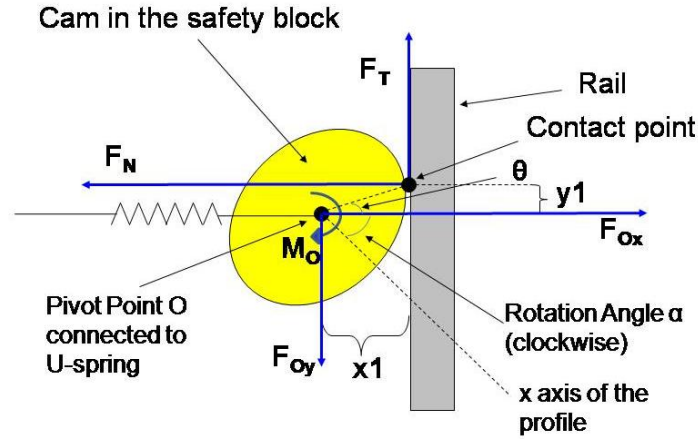


Figure 15. FBD of the selected Rotating Cam design

To analyze the motion of the cam, a free body diagram was created with all external forces (see Figure 15). For a given μ , the normal force should remain constant to exert a constant tangential force. When μ changes, then the cam will rotate and change its radius, thereby adjusting the normal force. Equilibrium conditions for a given μ yield the following equations:

$$\sum F_x = 0 \Rightarrow F_N = F_{Ox} \quad \text{where } F_{Ox} \text{ is the horizontal force provided at the pin by the U-spring} \quad (1)$$

$$\sum F_y = 0 \Rightarrow F_t = F_{Oy} \quad \text{where } F_{Oy} \text{ is the vertical reaction force at the pin} \quad (2)$$

$$\sum M_{pivot} = 0 \Rightarrow M_O = F_T x_1 + F_N y_1 \quad (3)$$

Numerical analyses employing the above equations were performed on several cam profiles using trial and error to obtain a profile that fit the desired deceleration range (see Appendix B.1 for the numerical analysis). Ultimately, an elliptical profile with a semi-major axis of 20 cm and semi-minor axis of 17.5 cm was found to have the best results.

Our original design called for the use of a torsion spring that would provide a relatively constant restoring moment M_o over the varying range of rotation of the cam. This posed a dilemma because industry torsion springs could not provide the high and constant restoring moment necessary for our design. Thus the design was modified to use a linear spring (the “restoring spring”) that would provide the restoring moment M_o . To accomplish this change, the spring will be attached at a fixed distance from the pivot to provide a sufficient moment arm on which the restoring spring can act.

5.3.2 Pin Diameter of Final Design

One major area of concern was shear stress acting on the pin. Consequently, a shear force analysis was performed to determine the pin diameter using Eq. (4). The maximum shear force at the pin was found to be 122,000 N, as calculated from the maximum reaction forces at the pin in the x- and y-direction using Eq. (5).

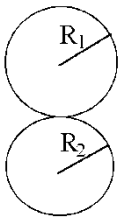
$$\tau = \frac{V}{A} \quad (4)$$

$$V = \sqrt{F o_x^2 + F o_y^2} \quad (5)$$

An approximate relation for shear yield stress based on tensile yield stress was used ($\sigma_{y, shear} \approx 0.58 \times \sigma_{y, tensile}$) and the shear yield stress of the cam pin was found to be 400 MPa if high-strength steel is used [3]. We added a safety factor of 3 and determined the pin diameter should be at least 3.5 cm.

5.3.3 Rack and Pinion Mechanism

We recognized that the contact area between the cam and the rail might be too small to dissipate the high heat and stresses that are experienced in elevator safeties. Based on Eq. (7)–(10) it was calculated that the maximum stress generated at the contact surface between the cam and the rail would be approximately $p_{max} = 740$ MPa [3] [4]. However, the yield strengths of steel and high-strength steel are only 448 MPa and 690 MPa, respectively, which are smaller than the possible maximum contact stress. In addition to the stress problem, it was determined that the contact area would be no larger than $2 \times 50 \text{ mm}^2$, which could lead to a heat dissipation problem.

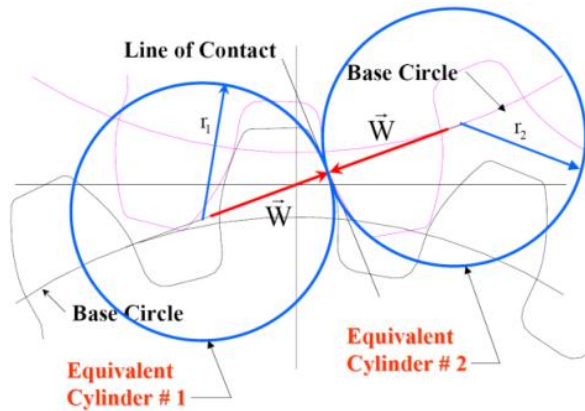


$$\frac{1}{R} = 1/R_1 + 1/R_2 \quad (6) \quad \frac{1}{E^*} = \frac{1 - \nu_1^2}{E_1} + \frac{1 - \nu_2^2}{E_2} \quad (7)$$

$$b = \sqrt{\frac{4F}{\pi L} \frac{1/E^*}{1/R_1 + 1/R_2}} \quad (8) \quad p_{max} = 2F / (\pi b L) \quad (9)$$

- $R_1 = 0.15$ m (minimum curvature of the cam profile)
- $R_2 = \text{infinity}$ (the rail is flat)
- $L = 0.05$ m (gear width)
- $\nu_1 = \nu_2 = 0.29$,
- $E_1 = E_2 = 200$ GPa (assuming both sides are made of steel)
- $F_{total} = 1.2 \times 10^5$ N (maximum total contact force)
- $b = \text{contact width}$ (due to deformation)

To resolve the issues of stress and heat, we incorporated a rack-and-pinion mechanism into our design. Figure 13 (p. 12) shows the brake shoe, which is placed between the cam and the rail. The brake shoe can slide vertically and horizontally within the frame; simultaneously, it contacts the cam via a set of teeth. Based on a simple free body diagram analysis, it was found that the contact forces between the rail and the brake shoe would be transmitted to the rotating cam through the rack and pinion mechanism (assuming that the weight of the brake shoe is negligible relative to the contact force exerted by the rail). The new design adds to the complexity of the system, but the physical principles remain the same.



$$r_1 = \frac{d_p \sin \phi}{2} \quad (10)$$

$$r_2 = \frac{d_g \sin \phi}{2} \quad (11)$$

$$C_p = \left[\frac{1}{\pi / E^*} \right]^{1/2} \quad (12)$$

$$\sigma_c = -C_p \left[\frac{W_t}{L \cos(\phi)} \left(\frac{1}{r_1} + \frac{1}{r_2} \right) \right]^{1/2} \quad (13)$$

- $d_p = \text{pinion pitch diameter}$
- $d_g = \text{rack pitch diameter}$
- $\phi = \text{pressure angle}$
- $C_p = \text{elastic coefficient}$
- $W_t = \text{tangential force}$

Figure 16. Equivalent contact cylinders for stress analysis [1]

For solving the stress problem, we used a typical gear model and analyzed the stress on the contact zone between the rack (cam) and pinion (sliding brake shoe). As shown in Figure 16 (p. 14), we can analyze the contact stress for the gear system using the same principle as the two-cylinder contact model that was discussed above. Equivalent radii r_1 and r_2 for the rack and pinion parts, respectively, can be calculated by Eq. (10) and (11).

After obtaining the contact width b , we applied Eq. (12) and (13) to get contact stress σ_c . Detailed parameter analysis (see Table 4) shows that the maximum contact stress is no larger than 470 MPa, which is significantly lower than with the pure cam design. Also, this contact stress value is much lower than the maximum σ_c that the current gears on the market (Carburized & Case Hardened 58-64 HRC) can bear, so the design is safe with respect to contact stress.

Properties	Symbol	Values	Units	Properties	Symbol	Values	Units
Rack Thickness	t	0.05	m	Tangential Force	W_t	17650	N
Pinion Pitch Diameter	d_p		m	Normal Force	W_n	118000	N
Gear Pitch Diameter	d_g	0.3	m	Contact Force	F	19475	N
Pressure Angle	ϕ	25	deg				
Equiv. Radius 1	r_1		m	Contact Stress	σ_c	462	MPa
Equiv. Radius 2	r_2	6.34×10^{-2}	m				
Stiffness of Rack	E_1	200	GPa				
Stiffness of Pinion	E_2	200	GPa				
Poisson's Ratio 1		0.29	/				
Poisson's Ratio 2		0.29	/				
Equivalent E	E^*	109.2	GPa	Gear found for max stress		Contact Stress	
Contact Width	b	5.37×10^{-4}	m	Carburized & Case Hardened		1896	MPa
Elastic Coefficient	C_p	1.86×10^5		58-64 HRC			

Table 4. Rack-and-pinion contact stress analysis

For analyzing the heat dissipation problem, we simply compared the new design to the current safety block. As long as the geometry of the brake shoe is similar to that of the current wedges, then it will dissipate heat sufficiently. This assessment is made assuming the material is the same and the current safety block can dissipate heat effectively.

5.4 Manufacturing Analyses

Specialized software was used to help determine the optimum materials, manufacturing processes, and assembly processes and to evaluate the safety and environmental impact of the final design.

5.4.1 Material and Manufacturing Process Selection

CES (EduPack 2007) software was utilized for material selection and processing (see Appendix L.1 and L.5 for a more detailed description). Because the cam and brake shoe are the two most vital parts of the new design, they were chosen for material analysis. Similar constraints were placed on both components, such as high compressive yield strength, low density, high working temperature, and low cost.

After specifying these constraints in CES, low alloy steel, AISI 8650 (tempered @ 425C, oil quenched) was chosen as the optimal material for the cam because of its affordability and high strength-to-density ratio. Ni-Cr white cast iron was chosen for the brake shoe because it meets the aforementioned requirements and because cast iron is used for the current brake shoe material.

CES's Manufacturing Process Selector was employed to help determine appropriate manufacturing processes. The cam can be formed using die casting, while the brake shoe should be investment casted. For both parts, the gear teeth are small enough that they have to be milled and each part requires a hole for sliding that will have to be drilled to attain higher precision. Because the yearly production volume for elevator safeties is large at 40,000 blocks, casting is the most economical method of manufacturing.

5.4.2 Design for Assembly

Rather than using software to optimize assembly, design for assembly charts (DFA) were employed (see Appendix L.2 for complete DFA charts). After assessing each component of the cam frame sub-assembly, it was determined that the nine parts could be reduced to seven parts by consolidating the brake shoe holder, brake shoe fastener, and brake shoe guide. As a result, the assembly time should take only 42 seconds, rather than 62 seconds, which equates to an efficiency improvement of 32%.

5.4.3 Design for Environment

Using SimaPro, a design for environment analysis was performed for the cast iron brake shoe and the high-strength steel cam (see Appendix L.3 for complete analysis). It was found that both materials have a similar effect in terms of life cycle assessment, with the high-strength steel having a slightly greater impact. Furthermore, it is evident that resources have a greater environmental impact than either the human health or ecotoxicity categories.

5.4.4 Design for Safety

To evaluate the safety risks of our prototype and final design, a risk assessment was performed for both models using DesignSafe software (see Appendix L.4 for a complete description). The risks for the prototype are minimal and relate mainly to the fabrication process because of the machinery involved. Once assembled, the forces in the prototype are relatively small and do not pose a high risk to the user.

On the contrary, the final design will have the responsibility of saving lives. Because death is the gravest consequence, it is important that the safety functions soundly. Thus, the heat and stress problems need to be addressed and analyzed extensively as these are the principal sources of failure. There will always be risk involved when working with elevator safeties, hence an acceptable risk approach was used. For critical components, a safety factor of 3 was established to quantify the balance between safety and cost-effectiveness.

6 PROTOTYPE DESCRIPTION

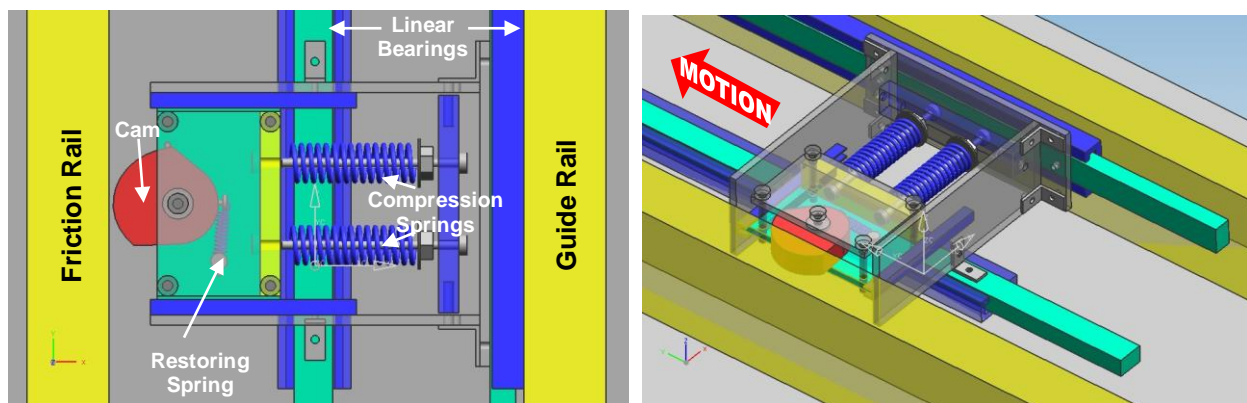


Figure 17. Top view (left) and isometric view of the CAD model for the prototype

The alpha prototype is a simplified, scaled-down version of the final design. Its main purpose is to validate the proposed design concept. The critical parameters for the prototype are different from the final

design, but the main function of a rotating cam remains the same. Figure 17 (p. 16) shows two views of the CAD model for the prototype. The following sections detail the prototype’s design features.

6.1 Design Simplifications

Since the goal of the prototype is to validate the rotating cam design, the secondary functions of the final design such as engagement are not included in the prototype. Other simplifications were also made to decrease the complexity of the system and to emphasize the rotating cam for demonstration purposes.

6.1.1 Horizontal Setup

Rather than dropping the safety along a guide rail, the prototype is pulled horizontally along a pair of guide rails. The mass of the prototype is supported entirely by linear bearings, such that the friction between the cam and the rail is the only tangential force. Therefore, the objective is to produce a constant tangential force, not a constant deceleration. In fact, the velocity of the prototype should remain constant during the demonstration. This setup allows the mechanism to operate under much smaller forces, on the order of 10 N in the tangential direction. Section 8.1 contains a full description of the physical validation plan.

6.1.2 Single cam

Instead of using two braking surfaces (one on either side of the rail) as in the final design, the prototype uses a single cam to generate a tangential force. As a result, there is only one braking surface. A set of bearings opposes the normal force of the cam without introducing a new friction force. To simplify the fabrication process, this reaction force will take place on a second rail, which is parallel to the original rail. The prototype rolls between the rails on a pair of linear slides.

6.1.3 Pre-engagement

The final design remains disengaged during normal elevator operation and will become engaged when the safety ropes are tensioned. This function is omitted for the prototype because of its complexity and because the engagement mechanism for the final design is similar to that of the current safety. For the prototype, the cam is engaged by tightening the compression springs using the thumb screws to provide a preloaded normal force.

6.2 Scaled Parameters

Several of the system parameters, including dimensions, spring constants, and forces, are scaled down to allow for easier fabrication and assembly. Table 5 enumerates the scaling of parameters for the prototype:

<i>Parameter</i>	<i>Full-Scale Design</i>	<i>Prototype</i>
Cam profile dimensions	20 cm × 17.5 cm	4 cm × 3.5 cm
Cam thickness	5 cm	1.9 cm
Normal force range	70.6–117.7 kN	25–33 N
Tangential force range	16.7–17.7 kN	9.27–9.81 N
Horizontal spring constant	1.82×10^7 N/m	90 N/m
Vertical spring constant	3.08×10^5 N/m	2.4 N/m
Friction coefficient	0.15–0.25	0.3–0.4

Table 5. Comparison of parameters for full-scale design versus prototype

6.2.1 Cam Profile Dimensions

The elliptical shape of the cam profile for the prototype remains the same as for the final design. It is scaled down to one-fifth the full size, making the semi-major dimension 4 cm and the semi-minor dimension 3.5 cm (see Figure 18, p. 18). These are the critical dimensions that affect the dynamic response of the system, thus the cam profile must fit this curve for all desired angles of rotation. The cam

is designed to rotate through 15° and this angle was expanded to 41.5° in case the range of μ increases. The remainder of the cam profile is subjective and was chosen to reduce material without compromising structural integrity. All other dimensions are designed to minimize the amount of required material.

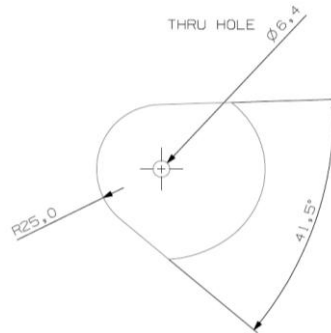


Figure 18. Cam profile for prototype

6.2.2 Spring Constants & forces

The full-scale springs for the final design are very stiff and require large preloads to achieve the desired forces. Even when these forces are scaled down by a factor of 5, the required normal force is still on the order of 10 kN, or roughly 1 ton. Clearly, this quantity is too high and poses assembly and safety issues. The forces have to be reduced further to allow for a more practical demonstration.

A target value of 10 N was established for the tangential force needed to pull the prototype along the guide rail. In order to achieve such a low value, other parameters had to be scaled. The mass that each full-scale safety has to stop at 0.6 g is 2,250 kg (5,000 kg / 2 blocks) for the full-scale design. For comparison, a tangential force of 10 N would be the equivalent of decelerating a falling 5 kg mass at 0.2 g. Because of the horizontal setup for the prototype, there is no mass that has to be stopped. This enabled us to choose a tangential force at our own discretion.

6.2.3 Materials & Friction Coefficients

The final design is made primarily of steel and cast iron to withstand the high forces. However, since the forces that the prototype experiences are much lower, aluminum was chosen as the material for most of the components because of its excellent machinability. The top cover for the cam frame is made of clear acrylic so that one can observe the cam's rotation. The remaining standard hardware is made from steel for its high strength and rigidity.

The guide rail can be composed of any material, but the coefficient of friction between the rail and the cam must be quantified. Consequently, both rails are wood beams and one can have different friction surfaces attached to it. Duct tape, packaging tape, and Teflon tape were selected as the surfaces that would be used for testing because they are easy to attach and they covered the desired range of μ . Simple experiments were conducted to determine μ values for these surfaces (see Section 8.1.1 for a description of these tests).

7 FABRICATION PLAN

The prototype was fabricated from both raw materials and standard parts. The custom parts must be machined from raw stock, whereas the standard parts can be assembled with little to no modification. See Appendix F for the Bill of Materials.

7.1 Custom Parts

The following parts are machined from raw stock material acquired from Alro Metals Plus in Ann Arbor, MI. See Appendix D for Dimensioned Drawings and Appendix G for Process Sheets. Additionally, see Appendix E for engineering change notices since Design Review #3.

- **ROTATING CAM** The cam is the most critical part of the prototype in terms of dimensions and tolerances. It is necessary to machine the cam in a CNC mill in order to achieve the complex curve. A scaled cam profile has been created in Unigraphics and the Computer Aided Manufacturing (CAM) feature aids in providing tool paths.

The remaining parts can be machined manually, primarily using a band saw and a drill press. Tolerances are less important for these parts.

- **PLEXIGLAS FRAME COVER** Anchors the rotating cam without obstructing one's view
- **ALUMINUM FRAME BASE** Anchors the rotating cam and vertical spring
- **ALUMINUM CASING SIDE WALLS** Provides a mounting surface for the U-channel
- **ALUMINUM CASING BACK WALL** Connects the side walls
- **CROSS MEMBER** Provides an anchoring surface for the compression springs

7.2 Standard Parts

The following parts are available in stock from McMaster-Carr (www.mcmaster.com) and require few to no additional modifications:

- **LINEAR BEARINGS** Standard drawer slides are attached to the two side rails and constrain the mechanism to movement along a single horizontal axis. They carry the entire weight of the prototype.
- **ALUMINUM U-CHANNEL** A U-channel provides the slot in which the cam frame can slide perpendicular to the rail.
- **CAM PIN** A standard 1/4"-20 screw is used as a pin about which the cam rotates. Only half of the screw is threaded, while the unthreaded length provides a smooth surface for contact with the cam pivot hole.
- **SPRINGS** Three springs are needed in all. Two horizontal compression springs press the cam frame against the rail, while one tension spring creates a moment on the cam.
- **THUMB NUTS** A thumb nut is a nut that is designed to be turned by hand. One thumb nut is placed on each spring guide screw; turning the thumb nut adjusts the preload on the horizontal spring.
- **2-HOLE CORNER BRACKETS** Two-hole corner brackets have been acquired to fasten together the case and to mount it to the bearings.
- **4-HOLE CORNER BRACKETS** Four-hole corner brackets have been acquired to fasten the rails to the base.

7.3 Assembly Instructions

The majority of the prototype is assembled using standard fasteners. The exceptions are the U-channels, which must be welded to the side walls. Screws cannot be used because they would impede the sliding motion of the frame in the slot. Care should be taken to not deform the interior of the U-channels during welding. Figure 19 (p. 20) illustrates the disassembled view of the cam frame sub-assembly and the overall assembly. Detailed assembly instructions follow.

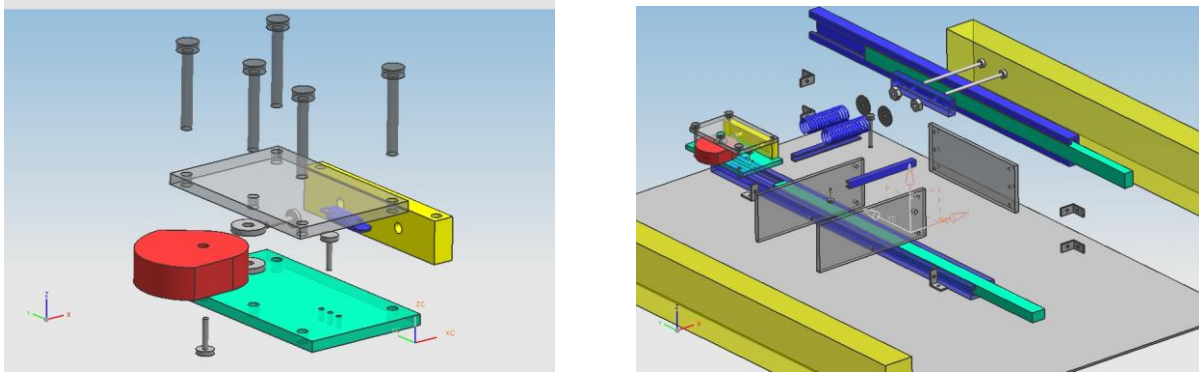


Figure 19. Exploded views of cam frame sub-assembly (left) and overall assembly

7.3.1 Cam Frame Sub-Assembly

- 1) Attach one end of extension spring to back of cam using 4-40 screw (no need to tighten screw)
- 2) Attach other end of extension spring to frame base via 4-40 screw and tapped holes
- 3) Fasten frame cover to frame wall with (2) 3/4" long 1/4"-20 screws
- 4) Slide 2" long 1/4"-20 3/4" thread screw through frame cover, (2) 1/4" ID washers, cam, (2) 1/4" ID washers, and frame base; tension must be put on extension spring; fasten with 1/4"-20 nut
- 5) Slide (2) 2" long 1/4"-20 screws through frame cover, frame spacers, and frame base; fasten with (2) 1/4"-20 nuts
- 6) Fasten frame base to frame wall with (2) 3/4" long 1/4"-20 screws

7.3.2 Casing Sub-Assembly

- 1) Weld 4" U-channel section to each of (2) side walls taking care to not deform the U-channel interior
- 2) Thread (2) 5" long 1/4"-20 screws through tapped holes on cross member
- 3) Thread thumb screw and slide fender washer onto each 5" screw followed by compression spring
- 4) Fasten side walls to back wall using (4) 2-hole corner brackets and (8) 10-24 machine screws with (8) lock washers
- 5) Fasten cross member to side walls using (2) 1/2" long 1/4"-20 screws

7.3.3 Base Sub-Assembly

- 1) Fasten (1) wood beam to plywood at 5" from one side using (3) 4-hole corner brackets and (12) wood screws
- 2) Mill 1/2" long slots in two adjacent holes in each of (3) 4-hole corner brackets
- 3) Fasten (1) wood beam to plywood at 5" from opposite side using (3) 4-hole corner brackets, (6) wood screws on beam, and (6) 10-24 screws with washers and T-nuts on plywood (slots in brackets face plywood)

7.3.4 Main Assembly

- 1) Drill (1) #16 hole in
- 2) Fasten (1) linear slide (narrow section) to casing back wall using (2) 8-32 screws
- 3) Fasten (1) linear slide (narrow section) to casing side walls using (2) 2-hole corner brackets, (4) 8-32 screws, and (2) nuts
- 4) Clamp prototype such that one linear slide is flush with the base and the other is flush with the fixed wood beam, making sure to line up slide ends with edge of base
- 5) Fasten (1) linear slide (wide section) to wood beam using (7) wood screws
- 6) Fasten (1) linear slide (wide section) to base using (7) wood screws
- 7) Attach duct tape/package tape/Teflon tape to brass sheet
- 8) Attach desired friction surface to rail using (2) spring clamps

7.4 Prototype Fabrication versus Final Design Manufacturing

Because the design of the prototype is much different from that of the final design, the fabrication process of each differs greatly. The final design will require mass production; therefore, individually machining each piece is undesirable. In terms of assembly, attaching the springs is much easier for the prototype because of the low forces. For the final product, the vertical spring will have to be attached to the cam with a large preload of approximately 70 kN. This installment will require machinery to achieve the necessary forces.

8 VALIDATION PLAN

Two approaches were used to validate our final design concept: physical and virtual. The physical validation was achieved with a scaled-down prototype that demonstrates the selected concept, while the virtual validation was done using ADAMS dynamic modeling software.

8.1 Physical Prototype Demonstration

The goal of the prototype is to physically validate the design concept. It is a scaled-down model, so the forces involved are much smaller; however, the concept remains the same. The prototype was tested by pulling the mechanism horizontally at a constant velocity using a force gauge (see Figure 20). Three different friction surfaces were interchanged and the resultant tangential force was measured for each.



Figure 20. Prototype validation concept

8.1.1 Determination of Friction Coefficients

Before testing the prototype across the friction surfaces, the coefficient of friction for each surface had to be determined. To do so, a mass (m) was dropped down an inclined plane with unknown surface friction coefficient μ (see Figure 21). The time required for the block to reach the bottom is a function of μ , the angle of incline (θ), and the distance traveled (d). Identical trials were performed for duct tape, packaging tape, and Teflon tape as the test surfaces.



Figure 21. Inclined plane experiment to determine μ for test surfaces with free body diagram (right)

A free body diagram yielded the following force balance equations:

$$\sum F_x : mg \sin \theta - F_f = ma ; (F_f = \mu F_N) \quad (14)$$

$$\sum F_y : F_N - mg \cos \theta = 0 \quad (15)$$

From these, the acceleration of the block was expressed in terms of the angle of incline, the coefficient of friction, and the acceleration of gravity:

$$a = g \sin \theta - \mu g \cos \theta \quad (16)$$

The distance traveled from rest given a constant acceleration is expressed by:

$$d = \frac{1}{2}at^2 \quad (17)$$

Finally, the acceleration was inserted into the above equation and μ was found in terms of the known parameters:

$$\mu = \tan\theta - \frac{2d}{t^2g \cos\theta} \quad (18)$$

The average time required for the aluminum block to reach the bottom of an inclined plane at a known angle was used to calculate μ for each of the three selected surfaces. The results are shown in Table 6.

Surface	μ
Teflon tape	0.20
Packaging tape	0.30
Duct tape	0.45

Table 6. Experimental coefficients of friction for 3 chosen surfaces

8.1.2 Prototype Test Results

Trials were repeated for the three friction surfaces (Teflon tape, packaging tape, duct tape) and the tangential force was measured for each (see Appendix H for complete test results). The initial lengths of the compression springs were also measured to ensure repeatability. The restoring extension spring length was increased from 1" to 1.5", which equates to a preload of 16.9 lb, and the compression spring length was decreased from 3" to 2.8125", equating to a preload of 2.1 lb.

The prototype was pulled with a force gauge the length of the linear slides (19") and the tangential force was recorded. Because the force readings did not stay constant for the entire travel length, readings were taken for the middle section of travel, which were generally lower than at the ends. It is important that the location of force measurement remains consistent. Tests were repeated with the cam's rotation restricted to show how the system performs without self-adjustment.

Preliminary tests across different surfaces clearly showed different angles of cam rotation, with the largest rotation occurring for the highest μ . The tangential force did not remain constant between surfaces but the percent variation was less than that of μ . Using $F_N = F_T/\mu$, the normal force was calculated and it was found that higher- μ surfaces showed a decrease in normal force, which is the desired qualitative response.

In order to produce a more positive quantitative response, the preload on the compression springs was adjusted until a quasi-constant tangential force was seen across different friction surfaces. Due to erratic force gauge readings, it was difficult to take force measurements with precision greater than 1 lb. However, even with this uncertainty, the tangential force with the rotating cam varied through a much smaller range than without the rotating cam. Average results for each of the three surfaces are shown in Table 7.

Surface	μ	Rotating cam		Fixed Cam	
		F_T (lb)	F_N (lb)	F_T (lb)	F_N (lb)
Teflon	0.20	3.0	15.0	3.3	16.5
Package Tape	0.30	3.3	11.0	4.4	14.7
Duct Tape	0.45	4.4	9.8	8	17.8

Table 7. Prototype test results showing improved stability in tangential force with the rotating cam

The above results show that for a 50% change in μ , from 0.2 to 0.3, the tangential force changes by only 10%, from 3.0 lb to 3.3 lb. Even more significant are the data found in the rightmost columns, which show results for testing with the cam fixed. The tests without the self-adjustment mechanism show three times the variation in tangential force and two-thirds the variation in normal force, as was anticipated

Overall, the physical tests were successful for the most part. They proved the concept functions as predicted by showing the decrease in normal force with an increase in μ and by showing the improvement in tangential force variation with the rotating cam. However, the numerical results did not align exactly with the theoretical calculations due to several sources of error, which are delineated in the Discussion section.

8.2 Virtual Dynamic Simulation

ADAMS simulates the dynamic components of the final design, including the two cams, the cam frames, the horizontal springs, the vertical springs, and an outer case that represents the elevator car (see Figure 22). The case is constrained to move along the vertical axis and the cam frames are constrained to move along the horizontal axis. The cams rotate about their centers with respect to the cam frames. The compression springs create a normal force between the case and the cam frames and the tension springs provide the restoring moment for the cams with respect to the cam frames.

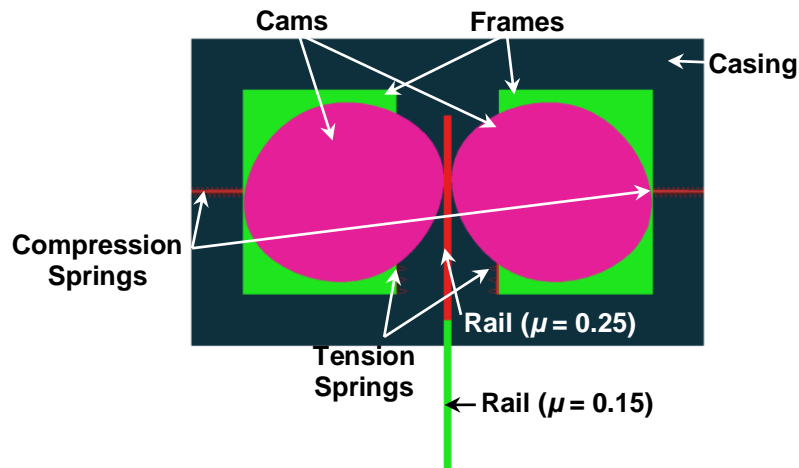


Figure 22. ADAMS component diagram

Each system component was assigned parameter values based on the analysis conducted in Excel. The system runs along two sections of rail, the first rail (top) with $\mu = 0.25$ and second rail (bottom) with $\mu = 0.15$. The simulation shows the rotation of the cams and plots the car velocity, car acceleration, and cam orientation versus time (see Figure 23, p. 24). As shown by the shaded area, the acceleration falls into the desired range of $5.88 \pm 0.49 \text{ m/s}^2$ or $0.6 \pm 0.05 \text{ g}$. The acceleration curve exhibits large spikes that are the result of the software trying to simulate a line contact. These anomalies take place over a single millisecond and do not impact the car's velocity, which remains a straight line.

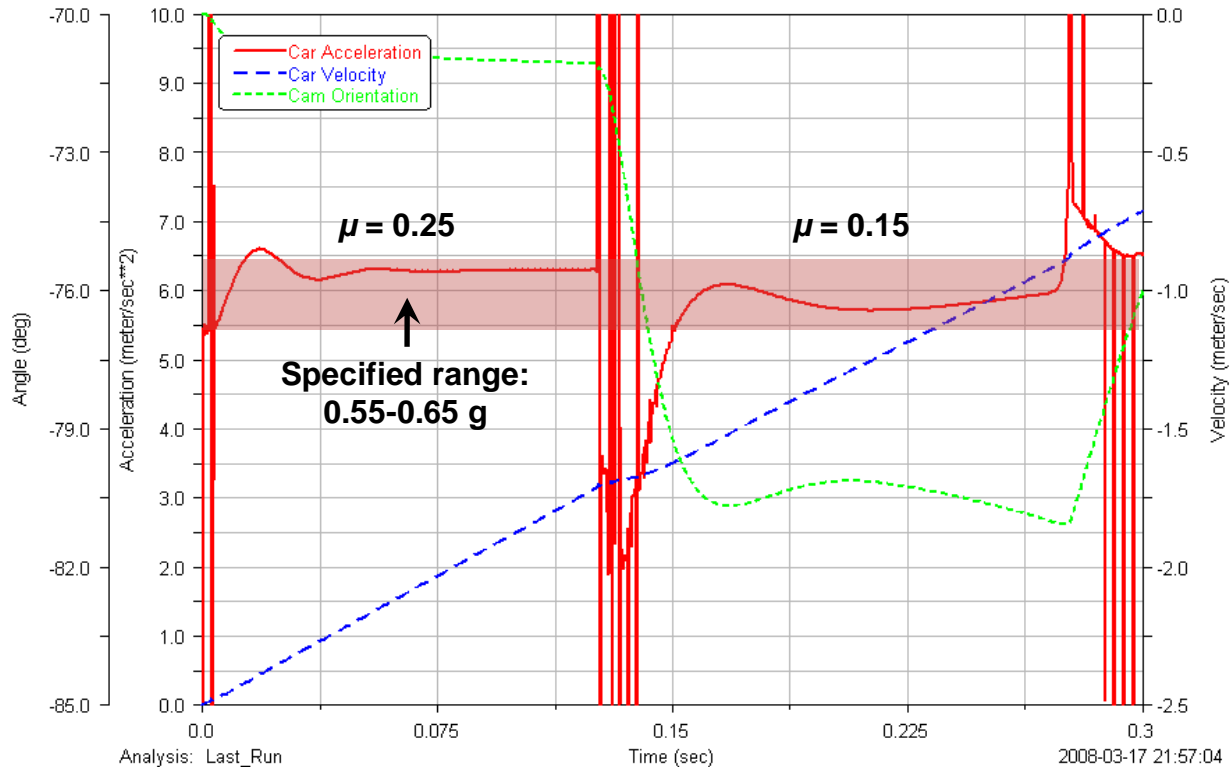


Figure 23. ADAMS simulation results of cam mechanism including car acceleration, velocity, and cam angle

It should be noted that the preloads for both the horizontal and vertical springs were adjusted from the calculated values in order to obtain the best results. Spring constants, however, were entered exactly as calculated.

9 DISCUSSION

The prototype proved the rotating-cam design concept to be functional; however, improvements in design of the prototype can be made to minimize error and improve validation. Sources of error include non-ideal friction interfaces (the friction across the test surface is not necessarily constant, there is friction on the linear bearings) and imprecise force measurements (it was difficult to pull the force gauge at a constant velocity).

Future experiments should eliminate additional friction as much as possible. For example, the shape distortion in the welded U-channels hindered the sliding motion of the cam system. For future prototypes, great care should be taken to avoid deforming the interior of the U-channel. A better alternative would be to use U-channels with a greater wall thickness so that they could be attached with countersunk screws to the casing without impairing the sliding motion. An even better solution would be to use a set of linear bearings to allow the cam frame to slide with minimal friction.

The major source of unwanted friction came from the linear slides, which exhibited more damping at the ends because drawer slides are designed to dampen at the ends. Bearings with a more uniform friction profile would produce more accurate readings, while bearings with less friction in general would further improve the accuracy.

As anticipated in Design Review #3, the springs used for the prototype presented issues. The standard springs used for the prototype do not exactly match the desired spring constants. Two compression

springs, both with spring constant $K_{spring} = 47$ lb/in, are used in the prototype producing an effective spring constant of $K_{effective} = 94$ lb/in. These are used in place of one compression spring with calculated spring constant $K_{calculated} = 90$ lb/in. Two extension springs with $K_{spring} = 2.1$ lb/in were used rather than one extension spring with $K_{calculated} = 2.4$ lb/in. This was necessary after it was found that one extension spring could not extend far enough to produce the desired force without yielding. As a result, two extension springs were used in parallel, thus doubling the spring constant to $K_{effective} = 4.2$ lb/in. This change likely compromised more accurate results and should be corrected for the next set of experiments. Future prototypes should utilize an extension spring with spring constant 2.1 lb/in that can withstand at least 6 lb of force (or 3" of extension).

Lastly, it would be helpful to measure the spring forces in the prototype. Currently, only the tangential force is measured, which can be used to calculate the normal force. It is possible to estimate the spring forces based on the nominal spring constants and approximate deflection, however this method is not very precise because of the high sensitivity of the compression springs. Using a separate force gauge to measure the force in the compression springs would make it easier to match the experimental spring forces with the calculated ones. This would in turn make it easier to optimize the spring adjustments to attain a constant tangential force.

10 FUTURE WORK

In addition to the recommendations mentioned in the previous section, higher-level work needs to be done to ensure the functionality of the full-scale design. Analysis should be done on the geometry (i.e. gear pitch) of the rack-and-pinion mechanism to optimize the amount of stress and heat dissipation. If necessary, alternatives should also be considered and developed because of the high risk involved with large forces.

An ADAMS model can be used to simulate the rack-and-pinion mechanism along with the engagement mechanism. A prototype with full-scale forces and final materials needs to be fabricated and tested to verify the final design. Contrary to the alpha prototype, the full-scale prototype should be tested by vertical freefall rather than horizontal pulling.

The current design is optimized to produce a constant deceleration for $0.15 < \mu < 0.25$; however, operation under a larger range of friction coefficients would make the design more robust. Hence, other more complex cam profiles should be explored. If the deceleration for a larger μ range becomes unstable, the locations of the spring attachments can be altered to change the force balance.

Finally, the current full-scale design is three times the size of the original safety. Because the volume has increased considerably, steps should be taken to minimize the weight of the casing. Rather than using solid plates, the outer casing can be changed to a skeletal structure so long as it can still hold the weight of the car without failing. A simple structural analysis can be performed to confirm this.

11 CONCLUSIONS

Our analyses and experiments have shown that the rotating-cam mechanism is a viable solution to the problem of varying rail friction during emergency stops. The rotating-cam mechanism automatically adjusts the normal force and renders it inversely proportional to the coefficient of friction, which results in a constant tangential force and constant deceleration.

The proposed concept has been manifested as a scaled-down prototype, which has been tested to establish physical validation. Tests were successful and it was found that the design functions as expected.

Although the tangential force was not kept constant, its range of variation was reduced to one-third the variation measure without the self-adjusting mechanism. The cam displayed a clear distinction in rotation angle between dissimilar friction surfaces. Furthermore, a virtual simulation of the full-scale design was created and shows that, for the specified friction range of $0.15 < \mu < 0.25$, the deceleration remains within the required deceleration range of 0.6 ± 0.05 g.

The rotating-cam concept has been analyzed and validated both physically and virtually. The next step is to develop the final design by examining the rack-and-pinion mechanism to help dissipate heat and stress. Once the geometry of the final design is optimized, a full-scale prototype can be fabricated and tested.

12 ACKNOWLEDGEMENTS

Our team would like to thank Nigel Morris, Jim Draper, and Anthony Cooney from Otis for sponsoring our project and for their professional guidance and technical advice on elevator safety systems.

We would also thank Bob Coury and Marvin Cressey from the ME450 machine shop, both of whom assisted us in our prototype fabrication. Bob was kind enough to operate the CNC mill for forming the cam and his welding experience was crucial for attaching our U-channels.

Thank you to Professor Sridhar Kota for his constructive opinions and for allowing us to borrow his force gauge for testing.

Finally, we would like to express our utmost gratitude to Professor Gregory M. Hulbert for his supervision and constructive feedback throughout the design process.

13 INFORMATION SOURCES

Most of the background information has come from Otis. We have conducted research, mostly using online databases, to find more information on elevator safeties and mechanisms. Literature searches and patent searches have yielded useful sources relating to our design concept.

13.1 Sponsor Information

The majority of our information comes directly from our sponsors at Otis. All technical specifications and design requirements were given by Nigel Morris in a project synopsis and then were expanded in a series of teleconferences [6]. Jim Draper, our technical advisor and mentor, provided us with benchmarking information in the form of elevator safety data during a dynamic event (Figure 3, p. 2) and engineering drawings (Appendix A). This information allowed us to get a sense of current elevator safety operation limits and physical dimensions.

The book *Elevator Mechanical Design* by Lubomir Janovsky [1] was given to the team and contains engineering information on all elevator subsystems including safeties. Otis also shipped an actual safety and section of guide rail to the team so we could investigate and understand the device we are redesigning.

13.2 Supplemental Materials

Further information was gathered in the form of a patent search and additional texts. The patent search allowed us to do further benchmarking on elevator safeties and was necessary to meet the customer requirement that our design does not infringe upon any current patents. The search yielded many patents on elevator safeties designs and materials that aided in concept generation [9]–[15]. As previously

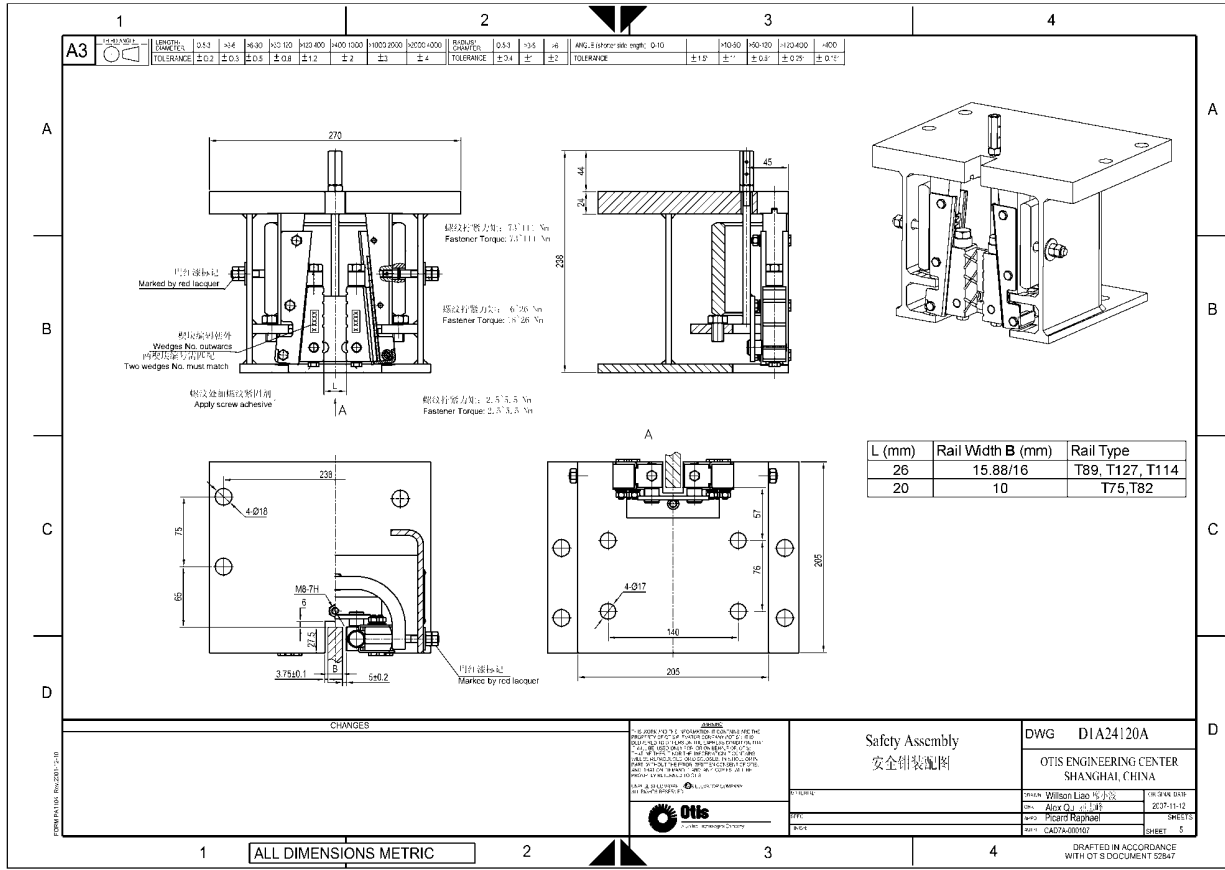
mentioned, it was discovered that at least one of our brainstormed concepts, the double-wedge design, has already been patented [12].

Depending on the design being developed, further information from textbooks was needed. The book *Cam Design Handbook* by Harold Rothbart was used to help develop cam profiles for the alpha design [16]. An online gear document allowed us to perform a stress analysis on the rack-and-pinion mechanism [1].

14 REFERENCES

- [1] LeMaster, R. A. "Involute Gear Tooth Contact Stress Analysis." Engineering 473 Class 20 lecture. *University of Tennessee at Martin*.
<<http://www.utm.edu/departments/engin/lemaster/Machine%20Design/Lecture%2022.pdf>>
- [2] Janovsky, L. (1999). *Elevator Mechanical Design (3rd ed.)*. Mobile, AL: Elevator World.
- [3] http://www.roymech.co.uk/Useful_Tables/Matter/shear_tensile.htm
- [4] <http://www.staff.ncl.ac.uk/s.j.bull/ecstr.html>
- [5] <http://www.mech.uwa.edu.au/DANotes/MST/contact/contact.html>
- [6] Morris, N. and J. Draper of Otis Elevator Company. Teleconference with Otis sponsors on 1/15/08, 1/29/08, and 2/12/08.
- [7] Emergency stop data from Otis
- [8] CAD Drawing from Otis
- [9] Ericson, R. J.; Cooney, A. Quasi-elliptical bidirectional progressive safety. U.S. Patent 5,931,263. 1999.
- [10] Osada, A. Braking Device for an elevator. U.S. Patent 5,363,942. 1994
- [11] Wikler, H.; Jong, J. Arrester device for elevators. U.S. Patent 4,819,765. 1989
- [12] Sasaki, H. Elevator emergency stopping device. U.S. Patent 6,997,287. 2006
- [13] Thompson, M.; Zatorski, R.; et al. Elevator safety brake having a plasma sprayed friction coating. U.S. Patent 5,964,322. 1999.
- [14] Thompson, M.; Beals, J. T.; et al. Carbon--carbon composite elevator safety brakes. U.S. Patent 5,979,615. 1999.
- [15] Thompson, M.; Beals, J. T.; et al. Molybdenum alloy elevator safety brakes. U.S. Patent 6,371,261. 2002.
- [16] Rothbart, H. (2004). *Cam Design Handbook*. New York, NY: McGraw-Hill.
- [17] Harris, T. "How Elevators Work," Howstuffworks.com.
<http://science.howstuffworks.com/elevator5.htm>, accessed 2/20/08.

APPENDIX A CURRENT SAFETY ENGINEERING DRAWING [8]



APPENDIX B SUPPLEMENTAL ANALYSES

B.1 Rotating Cam Design Analysis (Final Design & Prototype)

Final Design Product Setup		Analysis on U-spring (Horizontal)									
(assuming two safety blocks totally provide 0.6 g deceleration)		Angle (deg)	x1 (m)	y1 (m)	Stable mu	F_Normal (N)	F_Tangential (N)	F_T * x1 (N-m)	F_N * y1 (N-m)	M_Tors (N-m)	
Weight	2250.000 (kg)	70.0	0.1972	0.0153	0.250	70603	17651	3481	1078	4560	
SemiMajor	0.2000 (m)	72.5	0.1979	0.0136	0.208	82087	17061	3376	1116	4492	
SemiMinor	0.1750 (m)	75.0	0.1984	0.0118	0.182	92222	16752	3324	1089	4413	
Vertical Spring attached position		77.5	0.1989	0.0100	0.165	100888	16694	3320	1005	4325	
Height	0.2000 (m)	80.0	0.1993	0.0080	0.156	108003	16855	3359	869	4228	
x Length	0.1000 (m)	82.5	0.1996	0.0061	0.151	113658	17187	3430	691	4121	
Connect	0.1000 (m)	85.0	0.1998	0.0041	0.150	117672	17651	3527	480	4006	
Tangential Force Variance	-0.054	Analysis on torsion spring (or vertical counteracting spring)									
		Angle (deg)	Length (m)	Angle 2 (deg)	Moment arm (N-m)	Force (N)	Equiv. torque (N-m)				
U-Spring Constant	1.82E+07 (N/m)	70.0	0.2343	1.48	0.0948	48091	4560				
Vertical spring constant	3.08E+05 (N/m)	72.5	0.2301	1.15	0.0960	46808	4492				
		75.0	0.2259	0.86	0.0970	45510	4413				
		77.5	0.2217	0.61	0.0979	44200	4325				
		80.0	0.2174	0.40	0.0986	42879	4228				
		82.5	0.2131	0.23	0.0992	41549	4121				
		85.0	0.2087	0.10	0.0996	40212	4006				

Yellow Highlights indicate required spring constants

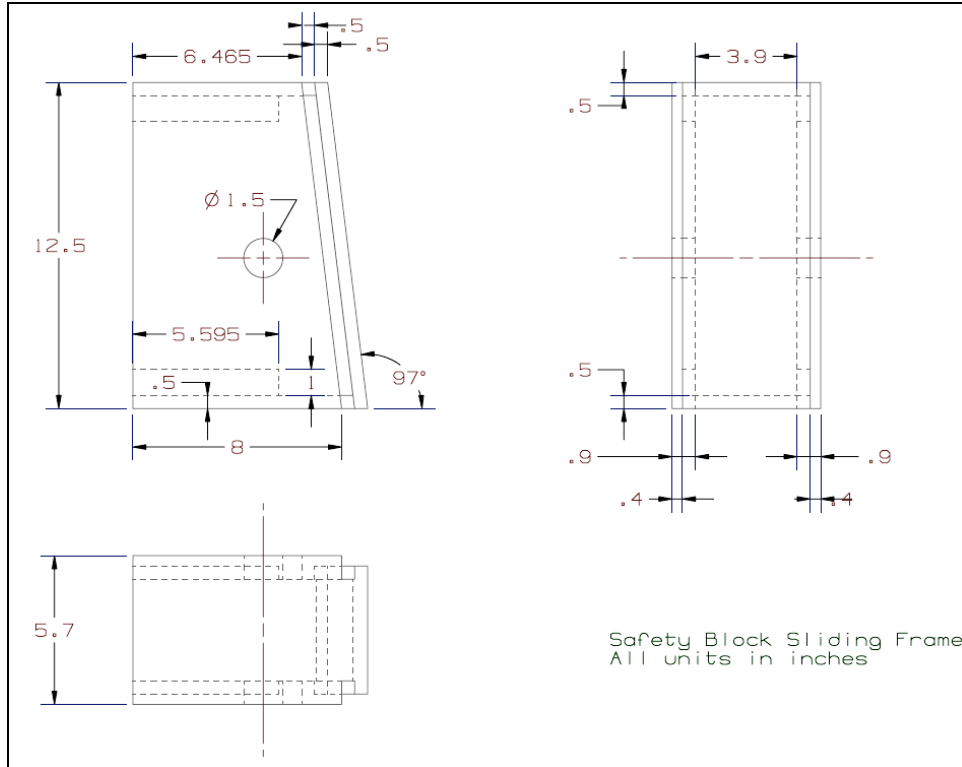
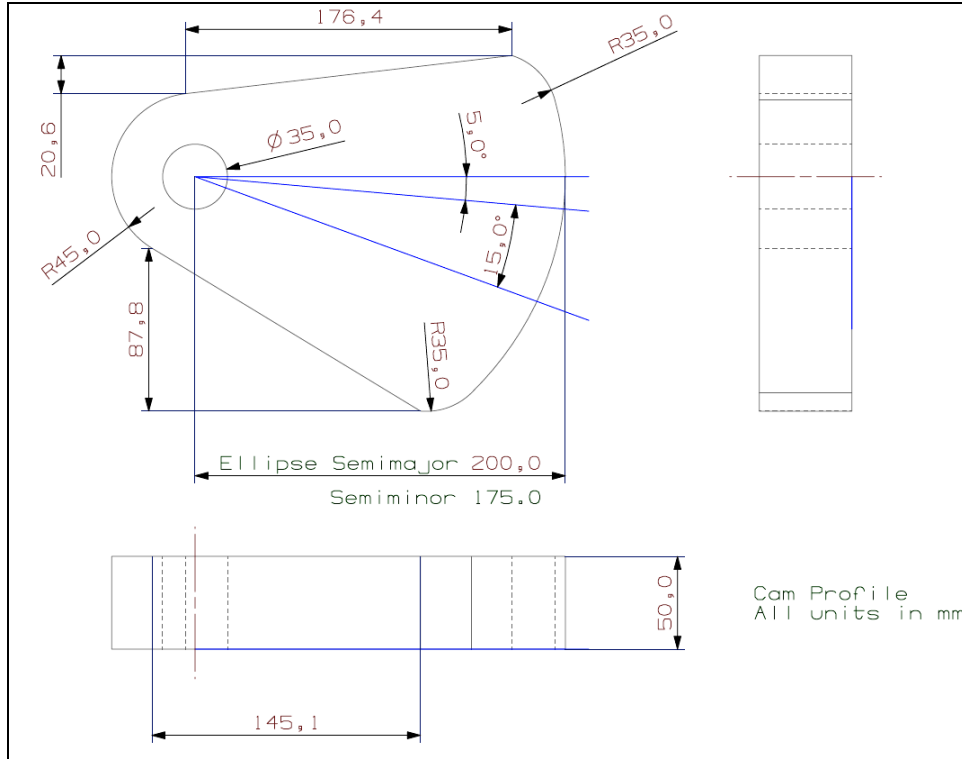
Proof-of-concept Prototype Design Setup		Analysis on U-spring (Horizontal)									
(assuming an acceleration of 0.2 g is generated)		Angle (deg)	x1 (m)	y1 (m)	Stable mu	F_Normal (N)	F_Tangential (N)	F_T * x1 (N-m)	F_N * y1 (N-m)	M_Tors (N-m)	
Weight	5.000 (kg)	70.0	0.0394	0.0031	0.250	39	9.81	0.387	0.120	0.507	
SemiMajor	0.0400 (m)	72.5	0.0396	0.0027	0.208	46	9.48	0.375	0.124	0.499	
SemiMinor	0.0350 (m)	75.0	0.0397	0.0024	0.182	51	9.31	0.369	0.121	0.490	
Vertical Spring attached position		77.5	0.0398	0.0020	0.165	56	9.27	0.369	0.112	0.481	
Height	0.0400 (m)	80.0	0.0399	0.0016	0.156	60	9.36	0.373	0.097	0.470	
x Length	0.0200 (m)	82.5	0.0399	0.0012	0.151	63	9.55	0.381	0.077	0.458	
Connect	0.0200 (m)	85.0	0.0400	0.0008	0.150	65	9.81	0.392	0.053	0.445	
Tangential Force Variance	-0.054	Analysis on torsion spring (or vertical counteracting spring)									
		Angle (deg)	Length (m)	Angle 2 (deg)	Moment arm (N-m)	Force (N)	Equiv. torque (N-m)				
U-Spring Constant	5.07E+04 (N/m)	70.0	0.0469	1.48	0.0190	27	0.507				
Vertical Spring Constant	8.56E+02 (N/m)	72.5	0.0460	1.15	0.0192	26	0.499				
		75.0	0.0452	0.86	0.0194	25	0.490				
		77.5	0.0443	0.61	0.0196	25	0.481				
		80.0	0.0435	0.40	0.0197	24	0.470				
		82.5	0.0426	0.23	0.0198	23	0.458				
		85.0	0.0417	0.10	0.0199	22	0.445				

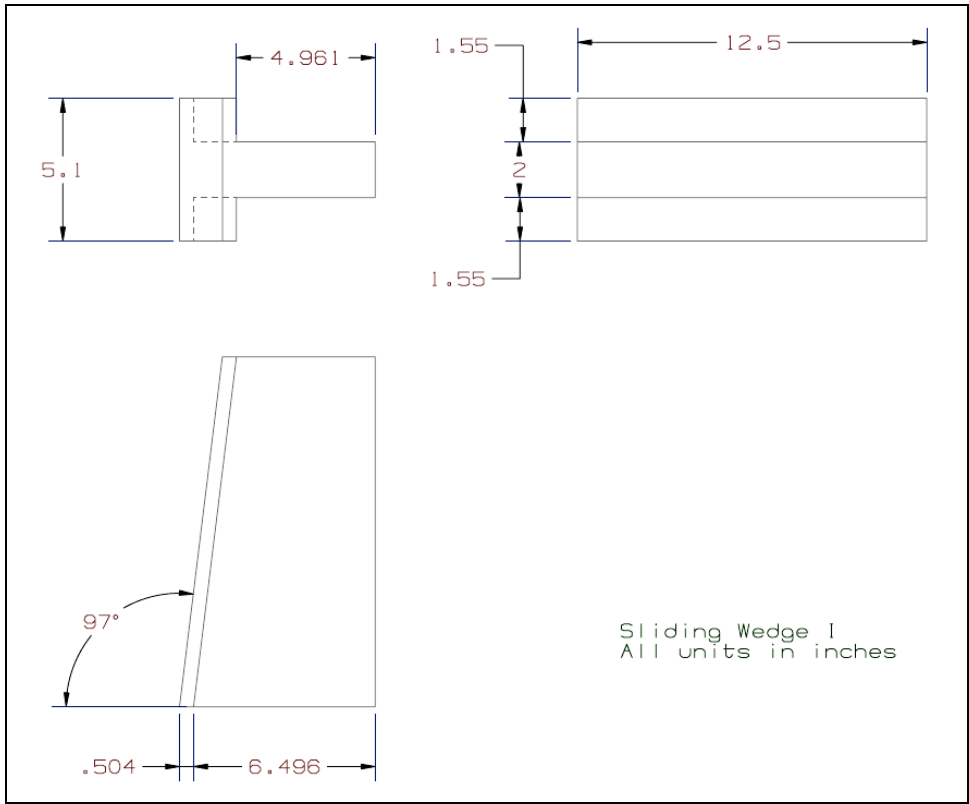
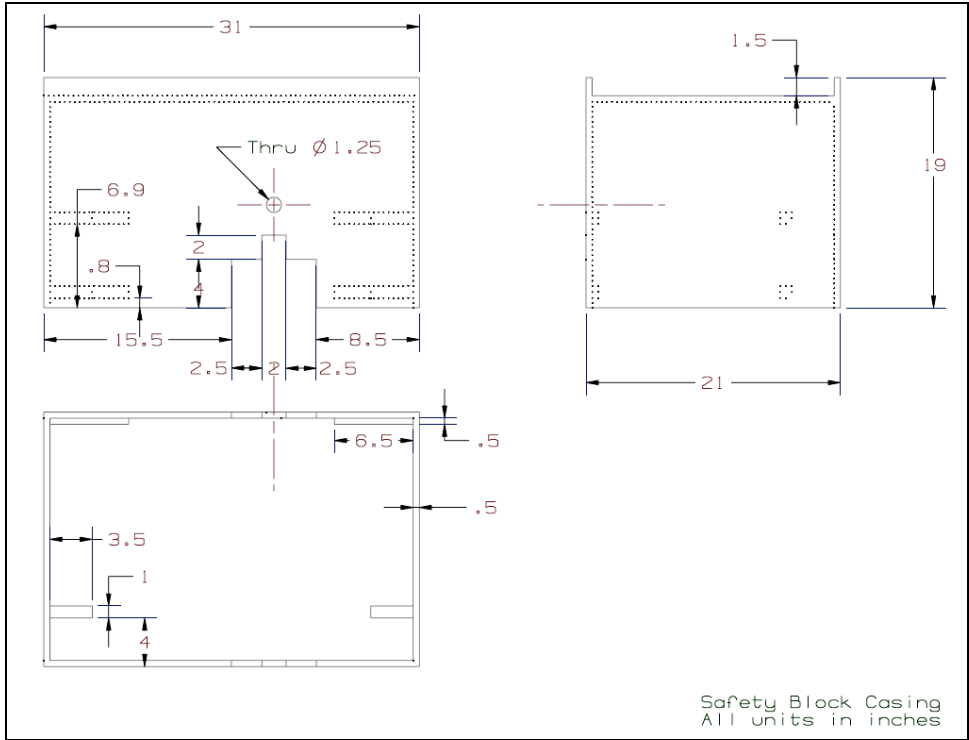
Yellow Highlights indicate required spring constants

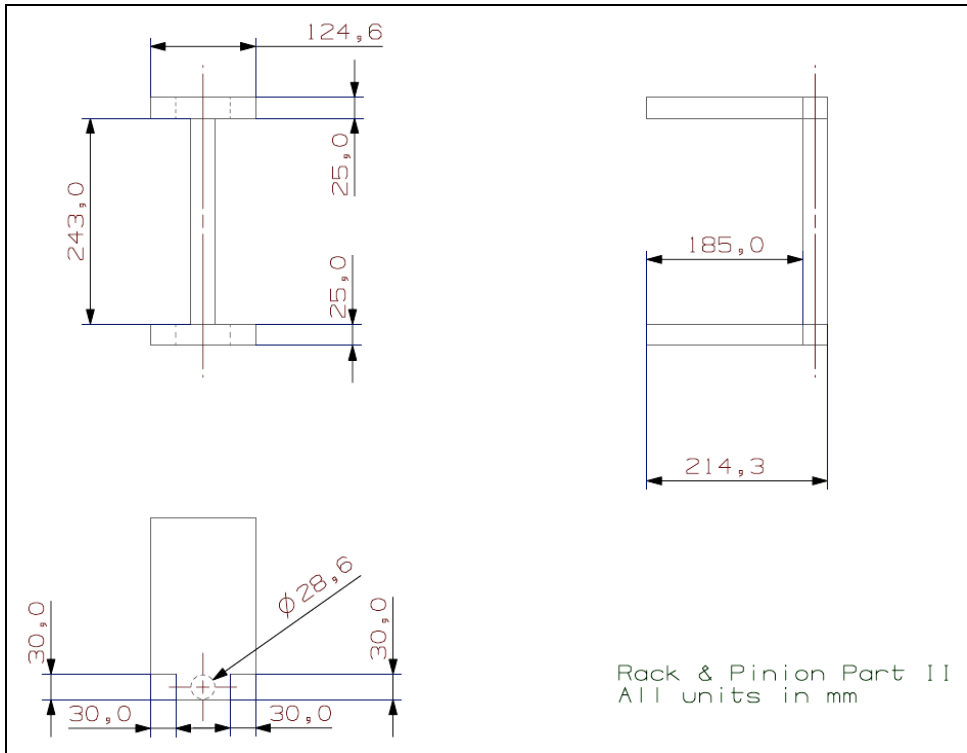
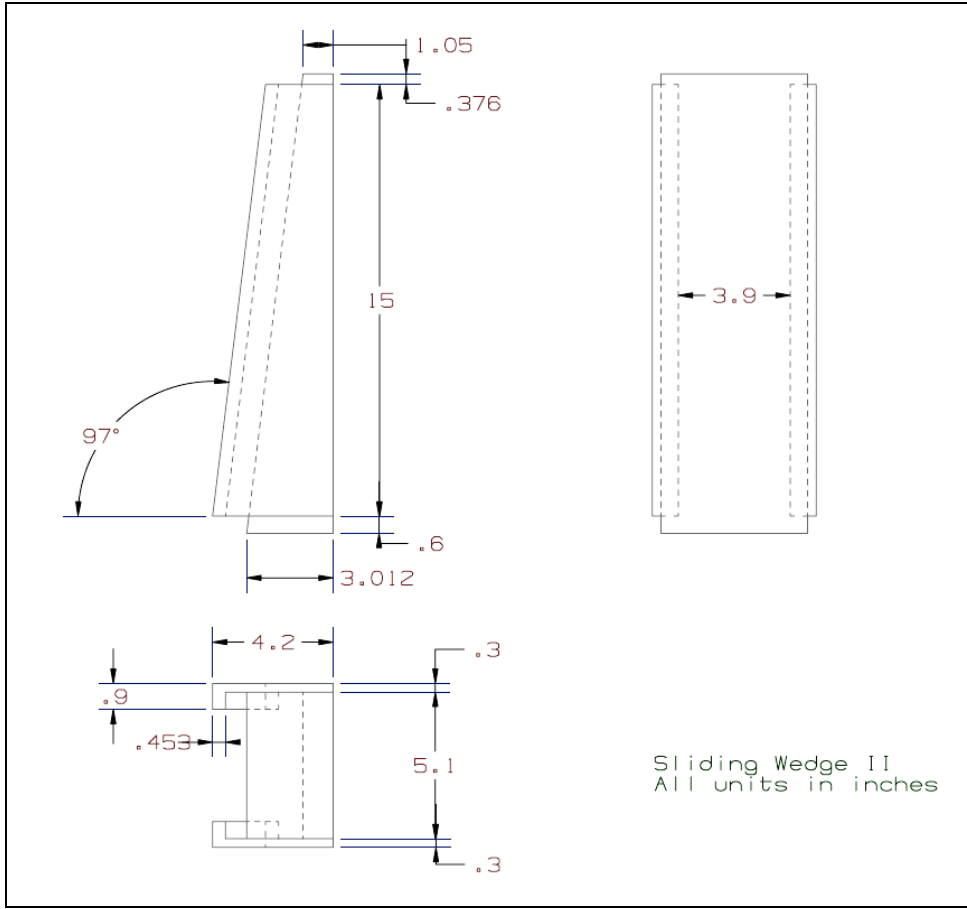
B.2 Screw in U-Spring Design Analysis

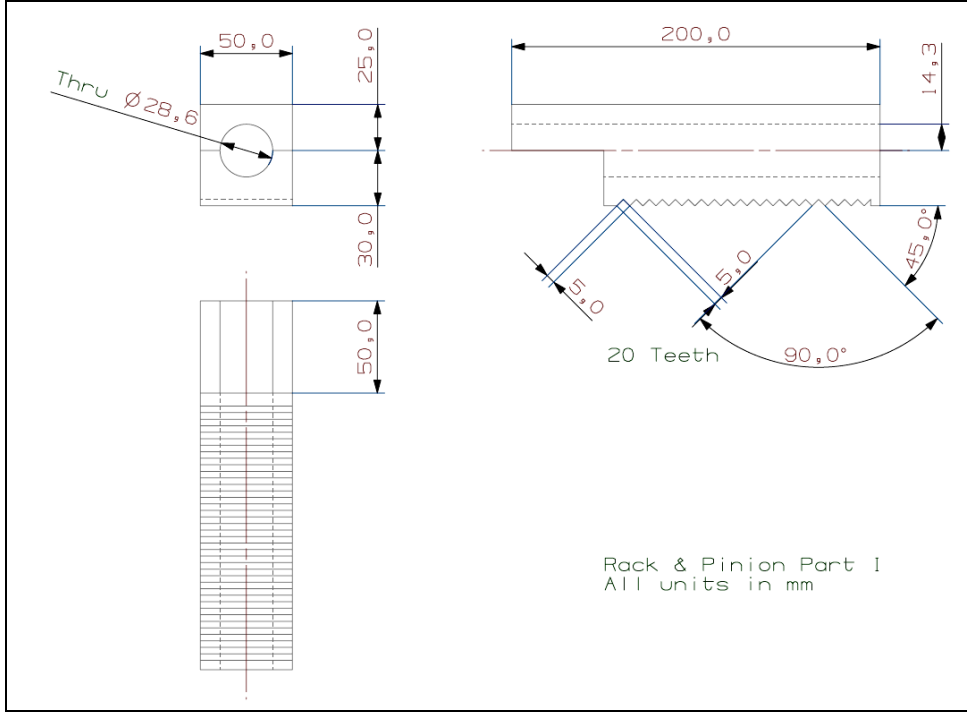
Car Parameters			Gib Parameters		
Mass	M	4500 kg	# surfaces	n	4 #
Accel	a	1.6 g	Tangential force	$F_T = M * a * g / n$	17650.8 N
Gravity	g	-9.806 m/s ²	Spring Parameters		
			Uspring constant	K_u	1.00E+07 N/m
			Vertical spring constant	K_v	8453.3142 N/m
			Target vertical spring constant		8453.3142
			Horizontal spring constant	K_h	500000 N/m
			Horizontal spring displ	x_h	0.01 m
			Horizontal spring force	$F_x = K_h * x_h$	5000 N
			Screw Parameters		
			Screw thread density	T_s	400 #/m
			Screw pitch	P_s	0.0025 m/rev
			Pinion diameter	D_p	0.01 m
			Rev per Δh	R_y	31.830989 rev/m
			Δd per Δh	N_p	-0.079577 m/m
Green cells indicate input parameters					
μ-Dependent Parameters					
Friction coeff	μ		0.15	0.2	0.25
Target Normal force	$F_N = F_T / \mu$		117672	88254	70603 N
Vertical spring force	$F_v = \mu * F_x$		750	1000	1250 N
Uspring displacement	$x = F_u / K_u$		0.01177	0.00883	0.00706 m
Uspring displacement at $\mu = .15$	$x_{.15}$		0.01177		m
Uspring displacement normalized to .15 value	$d = x - x_{.15}$		0	-0.00294	-0.00471 m
Vertical spring displacement normalized to .15 value	$h = d / N_p$		0	0.03697	0.059148 m
Vertical displacement at $\mu = .15$	$y_{.15} = F_{v_{.15}} / K_v$		0.08872		m
Vertical spring displacement	$y = h + y_{.15}$		0.08872	0.12569	0.147871 m
Vertical spring force	$F_v = K_v * y$		750	1062.5	1250 m
Uspring force	$F_u = K_u * x$		117672	88254	70603.2 N
Tangential force	$F_T = \mu * F_u$		17650.8	17650.8	17650.8 N

APPENDIX C FINAL DESIGN DIMENSIONED DRAWINGS









APPENDIX D PROTOTYPE DIMENSIONED DRAWINGS

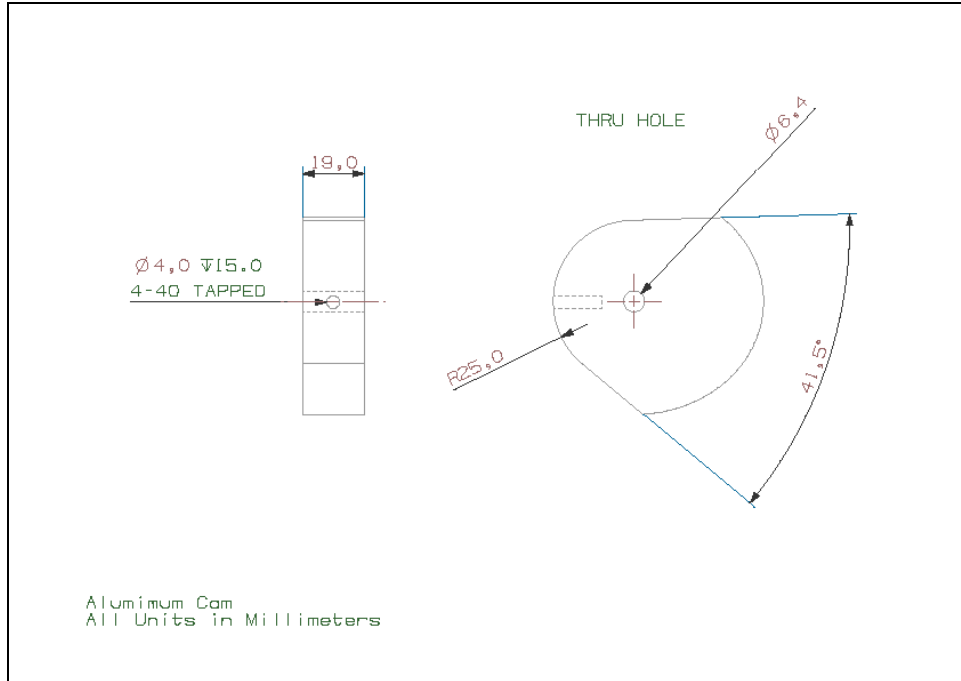


Figure 24. Cam

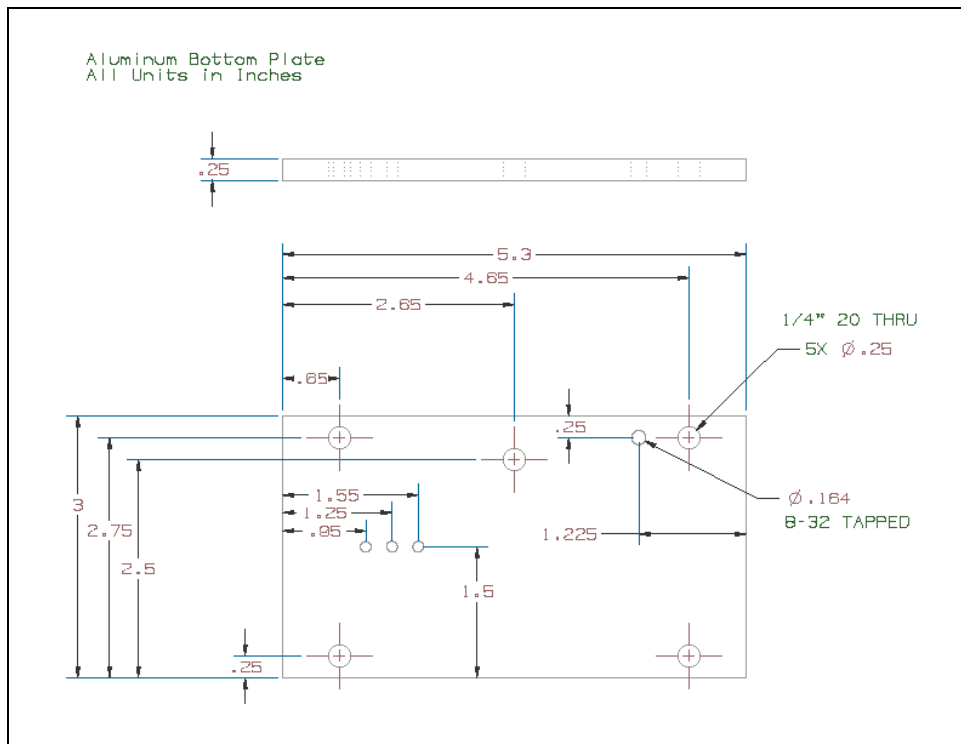


Figure 25. Frame base

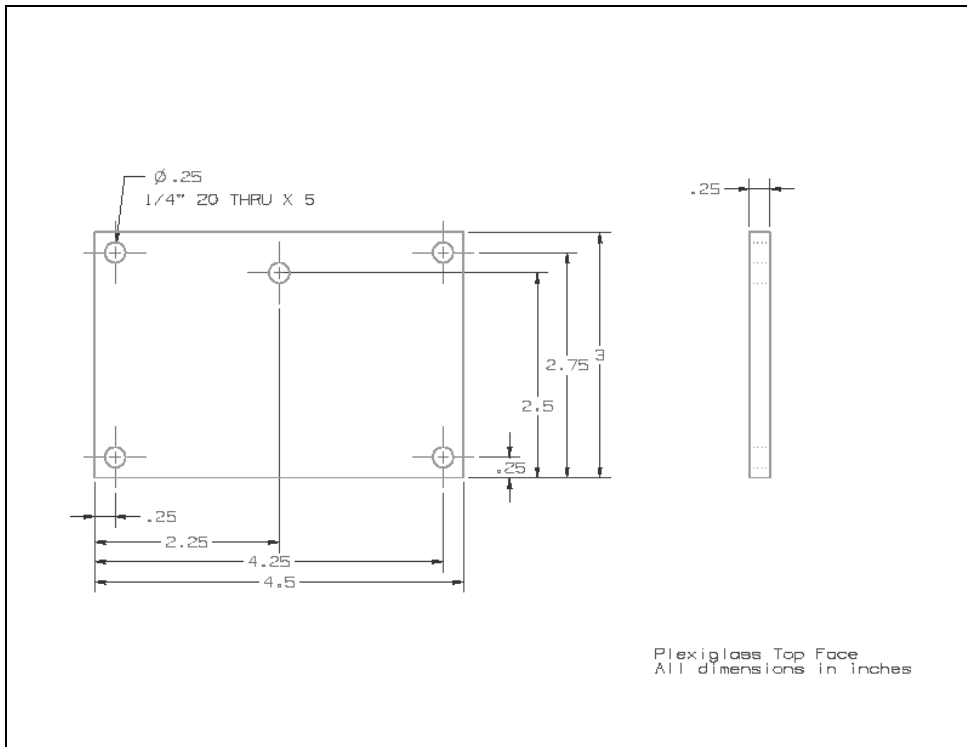


Figure 26. Frame cover

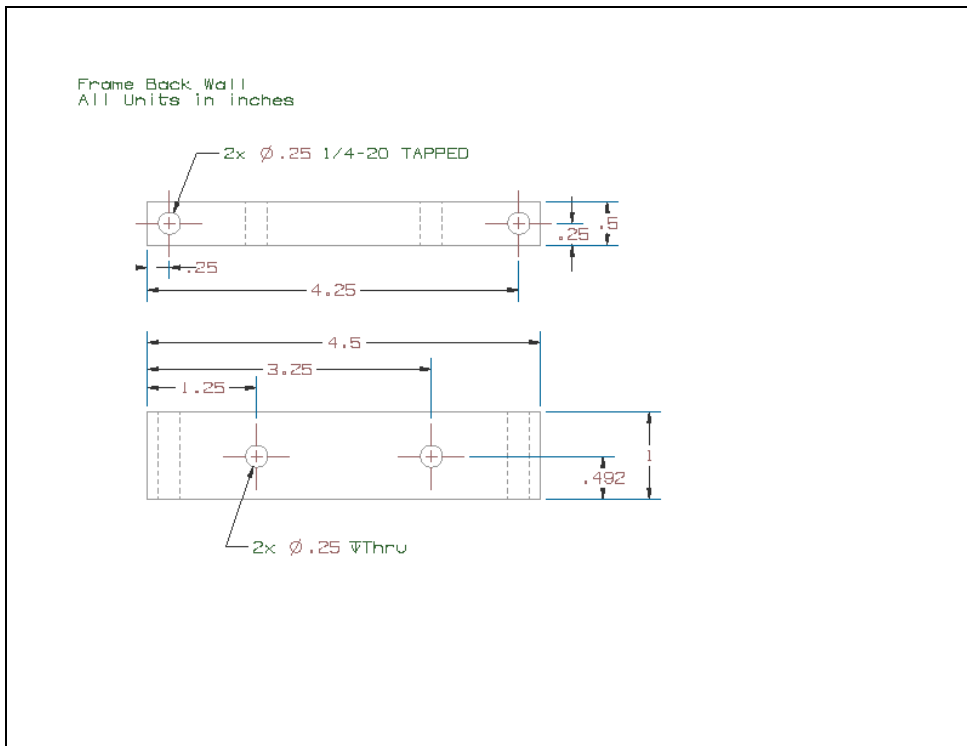


Figure 27. Frame back wall

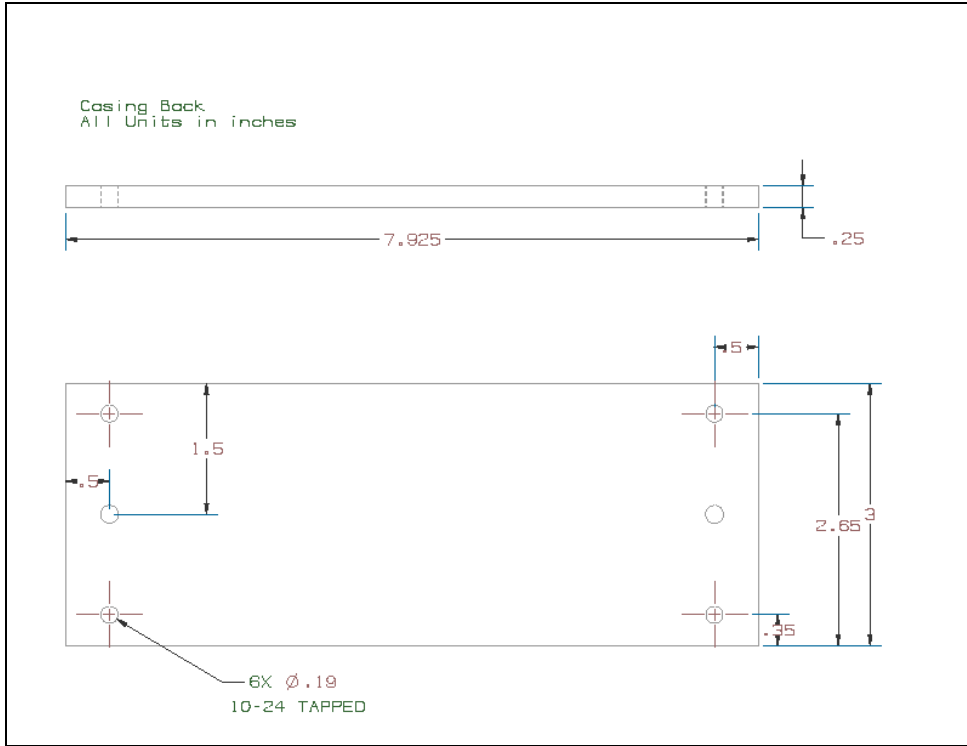


Figure 28. Casing back wall

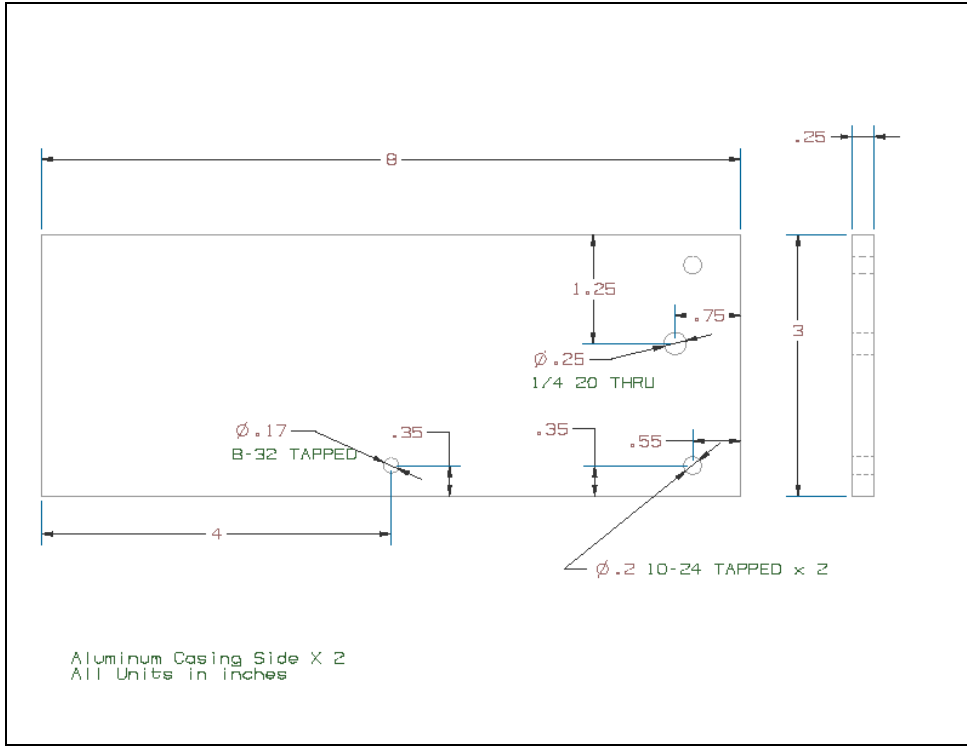
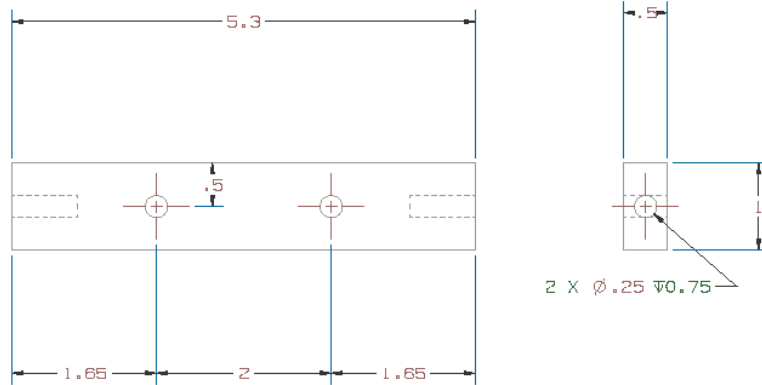


Figure 29. Casing side wall

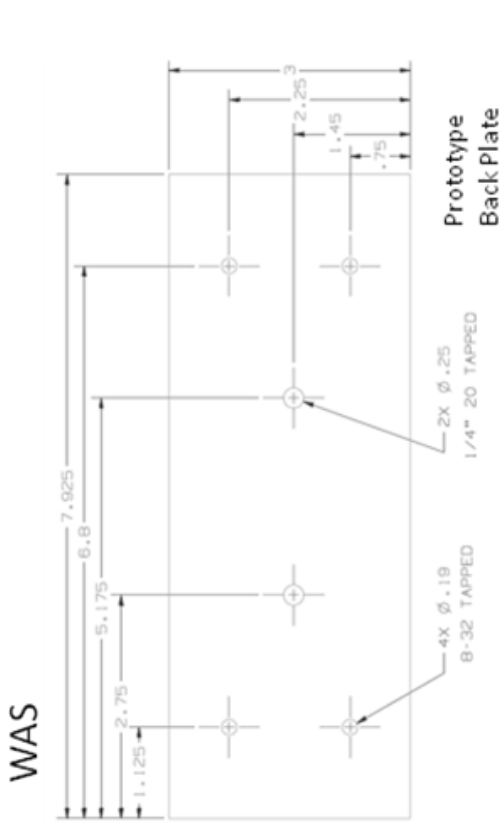
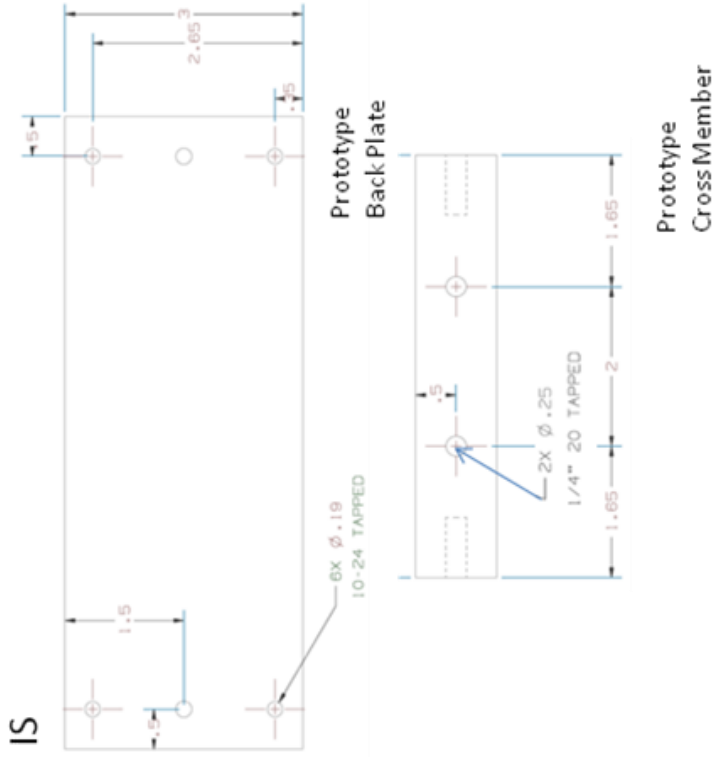


Frame Back Wall 11
 All Units in inches

Figure 30. Cross member

APPENDIX E ENGINEERING CHANGE NOTICES

Engineering Change Notice

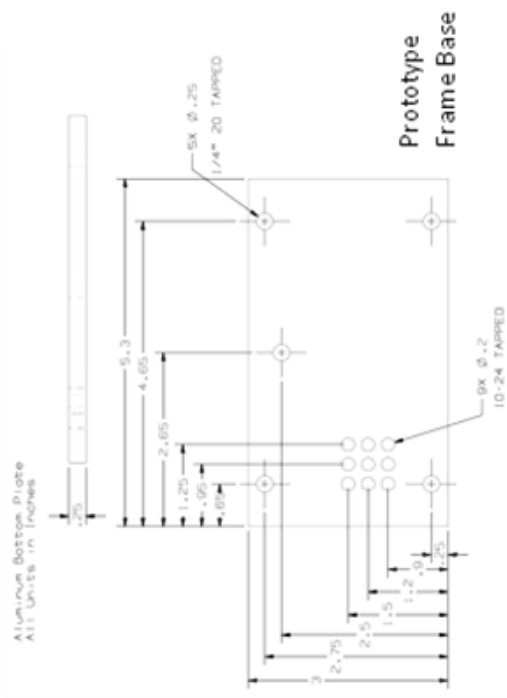


Notes:
 Needed to change the sizes and positions of 4 tapped holes at the corners of the back plate to fit angle brackets. Two 1/4" 20 tapped holes were removed but a cross member was added to attach the screws. Also, another two 10-24 tapped holes were added on the back plate for connecting the casing to the linear bearing.

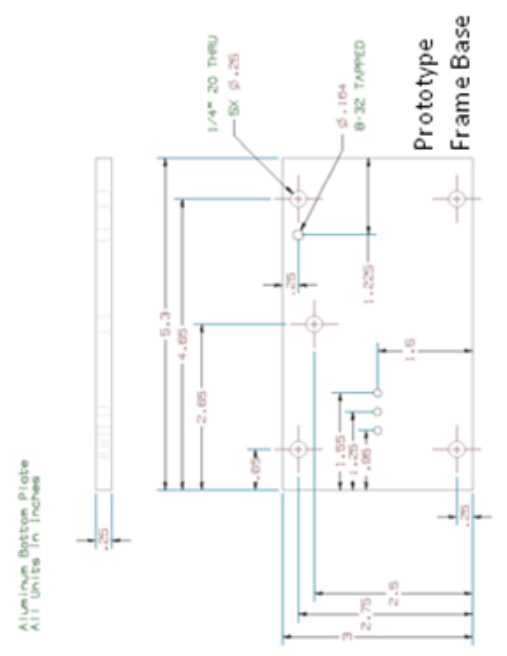
ME 450 Team 8, Sponsored by OTIS	
Project: Controlled Elevator Safety	
Ref Drawing: Prototype Back Plate	
Prototype Cross Member	
Engineer: M. Rayle, T. Zhang	3/22/2008
Engineer: J. Moss, M. Shek	3/23/2008

Engineering Change Notice

WAS



IS



Notes:

Eliminated bottom 2 rows of holes for spring attachment because they were determined to be superfluous

ME 450 Team 8, Sponsored by OTIS
Project: Controlled Elevator Safety
Ref Drawing: Prototype Frame Base
Engineer: M. Rayle, T. Zhang
3/22/2008
Engineer: J. Moss, M. Shek
3/23/2008

APPENDIX F BILL OF MATERIALS

Description	#	Purpose	Source	Part No.	Unit Price	UOM	Units	Price
3" x 1/4" BAR 6061-T651 CUT	1	Casing walls	ASAP	21437200	\$6.22	lb	3	\$18.66
1/4" (.220") PLATE ACRYLIC CLEAR LUCITE-CP TUFGARD	1	Frame cover	ASAP	AAA49500	\$3.00	EA	1	\$3.00
3/4" PLATE 6061-T651 ALUM CUT	1	Cam	ASAP	21440300	\$6.22	lb	1	\$6.22
1/2" X 1" RECT 6061-T6511 ALUM 36" PRE-CUT	1	Frame wall, cross member	ASAP	21438500	\$14.44	EA	1	\$14.44
304 SS Drawer Slide Friction Release, 26" L, 19" L Travel	2	Linear slides	McMaster	12155A36	\$68.49	Pair	1	\$68.49
Thumb Nut 1/4"-20 Screw, 23/64" O'all Height, 3/4" Head Dia	2	Spring adjustment	McMaster	93886A140	\$8.94	10-pk	1	\$8.94
Compression Spring 3" L, 1" OD, .120" Wire	2	Compression spring	McMaster	9657K21	\$10.63	6-pk	1	\$10.63
Extension Spring 1" L, 3/16" OD, .022" Wire	2	Restoring spring	McMaster	9432K26	\$6.24	6-pk	1	\$6.24
Corner Bracket Zinc-Plated, 7/8" Length, 5/8" Width	6	Corner brackets	McMaster	1556A24	\$0.34	EA	12	\$4.08
3/8"x3/8"x1/16" thick x 8' long U-channel	2	Frame sliding track (4")	Stadium Hardware		\$5.79	EA	1	\$5.79
Adjustable-pressure spring clamp	2	Friction surface attachment	Stadium Hardware		\$4.79	EA	2	\$9.58
1.5" x 10-24 eyehole hook	1	Force gauge attachment	Stadium Hardware		\$0.99	EA	1	\$0.99
1/4"-20 x 5" long hex-head screw	2	Spring guide	Stadium Hardware		\$0.60	EA	2	\$1.20
1/4" ID 1-1/4" OD fender washer	2	Spring contact interface	Stadium Hardware		\$0.18	EA	2	\$0.36
10-24 x 3/8" long machine screw	14	Casing fasteners	Stadium Hardware		\$0.07	EA	32	\$2.24
8-32 x 3/8" long machine screws/washers/nuts	4	Slide fasteners	Lowe's	57842	\$0.98	20-pk	1	\$0.98
2"x4"x7" wood beam	2	Guide rails (36")	Lowe's	6004	\$1.55	EA	1	\$1.55
1/4"-20 x 2" hex-head screw, 3/4" thread	1	Cam pin	Lowe's	63313	\$0.14	EA	1	\$0.14
36" x 24" x 1/2" thick plywood	1	Base	Shop					
4 hole corner brackets	6	Rail brackets	Shop					
1/2" OD x 1/4" ID x 1" long aluminum tube	2	Frame spacers	Shop					
10-24 T-nuts	6	Bracket fastener (1 side)	Shop					
1/4"-20 x 3/4" hex-head screw	4	Frame cover/base fasteners	Shop					
1/4"-20 x 2" hex-head screw	2	Frame fasteners	Shop					
1/4"-20 x 1/2" brass hex-head screw	2	Cross member fasteners	Shop					
1/4"-20 nut	3	Frame fasteners	Shop					
1/4" washer	4	Cam spacers	Shop					
8-32 x 1" machine screw	1	Cam rotation restrictor	Shop					
8-32 nut	4	Cam rotation restrictor	Shop					
1/4" lock washer	14	Casing fasteners	Shop					
10-24 washer	6	Base fasteners	Shop					
4-40 x 1/2" machine screw	3	Restoring spring attachment	Shop					
1/2" wood screws	30	Base fasteners	Shop					
washers	6	Base fasteners	Shop					
24" x 1.5" brass sheet	3	Friction surface sheets	Shop					
2" Duct tape		Friction surface (24")						
2" Packaging tape		Friction surface (24")						
1/2" Teflon tape		Friction surface (24")						
Total cost								\$163.53

APPENDIX G PROTOTYPE PROCESS SHEETS

Part	Cam	Component	Cam			
Stock	4" x 4" x 3/4" aluminum sheet					
No.	Description	Machine	Tool	Speed	Fixture	
1	Mount stock	CNC mill	N/A	N/A	Vise	
2	Drill 15/64" hole	CNC mill	15/64" drill	1400 rpm	Vise	
3	Set the origin at hole	CNC mill	N/A	N/A	Vise	
4	Ream 1/4" hole	CNC mill	1/4" ream	200 rpm	Vise	
5	Drill (2) 1/4" holes at (0.5, ± 0.5) from the origin	CNC mill	1/4" drill	1400 rpm	Vise	
6	Fix the raw piece on a base using 1/4" screws and mount the base onto CNC vise	CNC mill	N/A	N/A	Vise	
7	Zero origin	CNC mill	Edge Finder	1400 rpm	Vise	
8	Run program	CNC mill	1/4" drill	1200 rpm	Vise	
9	Drill #7 hole on back curved face thru to pin hole	Drill press	#7 drill	2500 rpm	Vise	
10	Tap hole on back for spring attachment screw	Hand tap	1/4-20 tap	N/A	Vise	

Part	Frame base	Component	Cam frame			
Stock	5.3" x 3" x 1/4" Aluminum sheet					
No.	Description	Machine	Tool	Speed	Fixture	
1	Drill 1/4" hole for pin 1/2" from top at center	Drill press	1/4" drill	2000 rpm	Vise	
2	Drill (4) 1/4" holes for mounting screws 1/4" from top/bottom 0.65" from sides	Drill press	1/4" drill	2000 rpm	Vise	
3	Drill (4) #43 holes for spring attachment .95" from side at center, spaced .3"	Drill press	#43 drill	2000 rpm	Vise	
4	Drill #29 hole for cam rotation pin at 1.225" from right side, 1/4" from top	Drill press	#29 drill	2000 rpm	Vise	
5	Tap spring attachment holes	Hand tap	4-40 tap	N/A	Vise	
6	Tap cam rotation pin hole	Hand tap	8-32 tap	N/A	Vise	

Part	Frame cover	Component	Cam frame			
Stock	6" x 3" x 1/4" Plexiglas sheet					
No.	Description	Machine	Tool	Speed	Fixture	
1	Cut length to 4.5"	None	Saw	N/A	Vise	
2	Drill 1/4" hole for pin 2.5" from bottom at center	Drill press	1/4" drill	1000 rpm	Vise	
3	Drill 1/4" thru holes 1/4" from edges for mounting screws	Drill press	1/4" drill	1000 rpm	Vise	

Part	Frame back wall	Component	Cam frame			
Stock	1" x 1/2" aluminum bar					
No.	Description	Machine	Tool	Speed	Fixture	
1	Cut length to 4.5"	Band saw	N/A	1000 fpm	None	
2	Drill (2) #7 thru holes on 1/2" face 1/4" from edges	Drill press	#7 tap drill	2000 rpm	Vise	
3	Drill (2) 1/4" thru holes 1.25" from edges	Drill press	1/4" drill	2000 rpm	Vise	
4	Tap (2) outer-most holes	Hand tap	1/4"-20 tap	N/A	Vise	

Part	Back plate	Component	Casing			
Stock	8" x 3" x 1/4" aluminum sheet					
No.	Description	Machine	Tool	Speed	Fixture	
1	Drill (6) #25 thru holes at 0.35", 1.5", 2.65" from bottom, 0.5", 2.5" from left side for corner brackets	Drill press	#25 drill	2500 rpm	Vise	
2	Tap (6) holes	Hand tap	1/4"-20 tap	N/A	Vise	

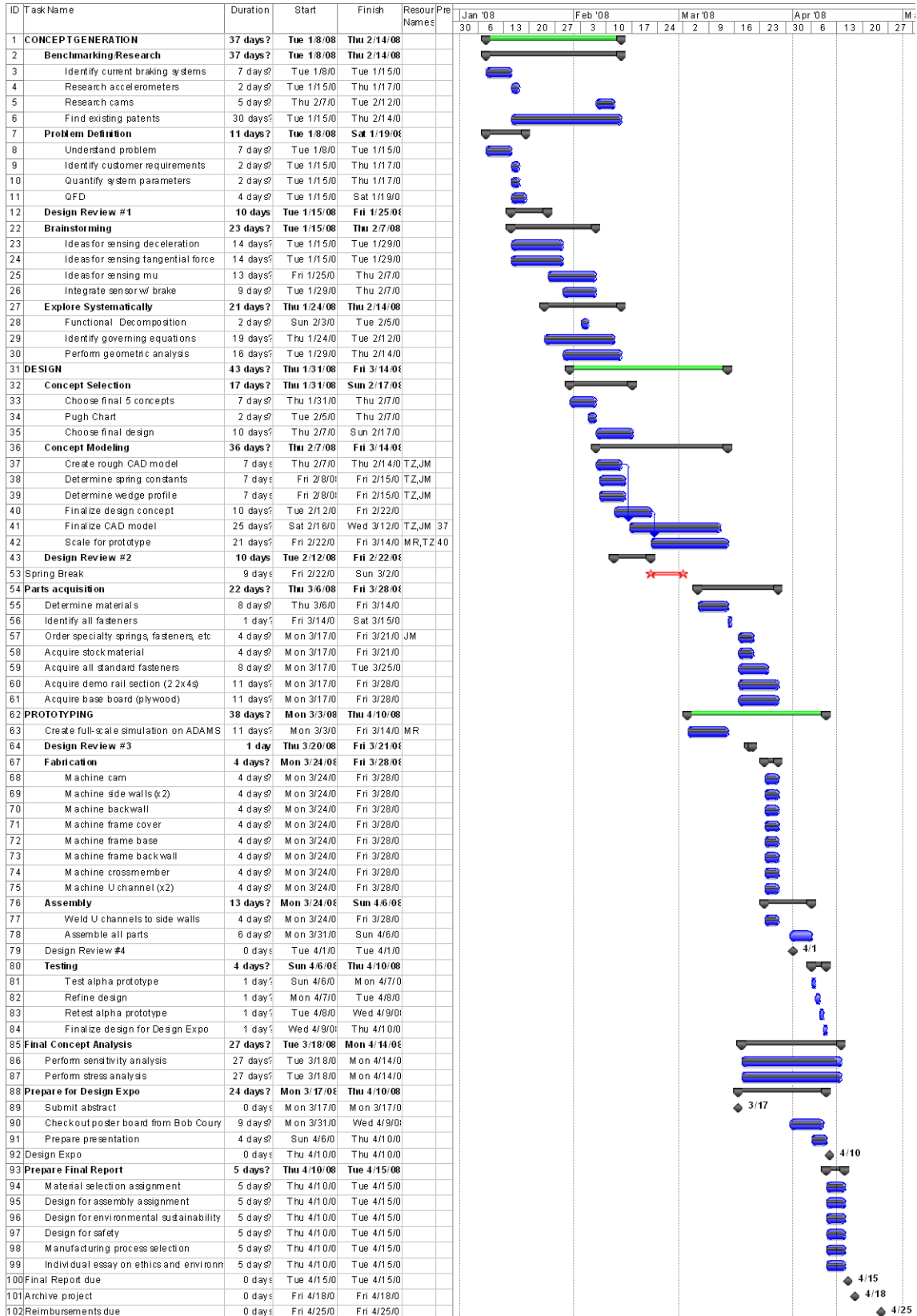
Part	Side plate (x2)	Component	Casing			
Stock	8" x 3" x 1/4" aluminum sheet					
No.	Description	Machine	Tool	Speed	Fixture	
1	Drill (2) #25 holes at 0.55" from right side, 0.35" and 2.65" from bottom for corner brackets	Drill press	#25 drill	2000 rpm	Vise	
2	Drill #29 hole at 0.35" from bottom at center for slide mount	Drill press	#29 drill	2000 rpm	Vise	
3	Drill 1/4" hole 2.75" from bottom, 0.75" from right side for cross member	Drill press	1/4" drill	2000 rpm	Vise	
4	Tap (2) corner bracket holes	Hand tap	10-24 tap	N/A	Vise	
5	Tap slide mount hole	Hand tap	8-32 tap	N/A	Vise	

Part	Cross brace	Component	Casing			
Stock	1" x 1/2" aluminum bar					
No.	Description	Machine	Tool	Speed	Fixture	
1	Cut length to 5.3"	Band saw	Saw blade	1000 fpm	None	
2	Drill (2) #7 holes at 1.65" from ends at center in 1" face for spring screws	Drill press	#7 drill	2000 rpm	Vise	
3	Drill (2) #7 holes 0.75" deep on each end face at center for mounting	Drill press	#7 drill	2000 rpm	Vise	
4	Tap (4) holes	Hand tap	1/4"-20 tap	N/A	Vise	

APPENDIX H COMPLETE TEST RESULTS

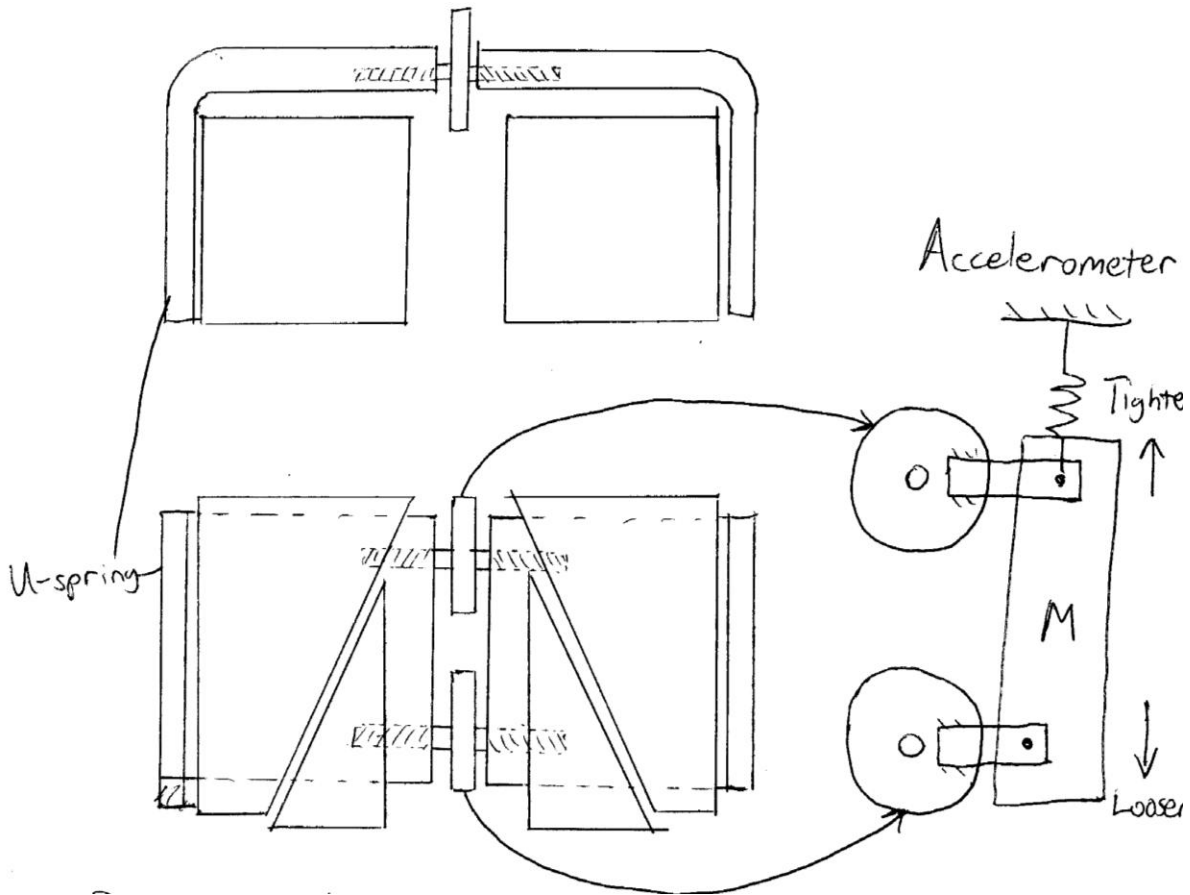
Horizon. Spring Constant	90	lb/in	Horizon. Spring Original Length	3.00	in
Vertical Spring Constant	4.2	lb/in	Vertical Spring Original Length	1.00	in
Horizontal Spring Preload Length	2.625	in			
Vertical Spring Preload Length	1.5	in			
	μ				
Teflon	0.20	4.5	Pulling Force w/o Self-adjusting	22.5	Normal Force w/o Self-adjusting
Duct Tape	0.45	5.2	Theoretical	4.50	Theoretical
% Change	125	16	Experimental	10.13	22.5
					22.5
				11.6	
Horizontal Spring Preload Length	2.75	in			
Vertical Spring Preload Length	1.5	in			
	μ				
Teflon	0.20	3.8	Pulling Force w/o Self-adjusting	19.0	Normal Force w/o Self-adjusting
Duct Tape	0.45	5.0	Theoretical	3.80	Theoretical
% Change	125	32	Experimental	8.55	19
					19
				11.1	
Horizontal Spring Preload Length	2.8125	in			
Vertical Spring Preload Length	1.5	in			
	μ				
Teflon	0.20	3.0	Pulling Force w/o Self-adjusting	15.0	Normal Force w/o Self-adjusting
Package Tape	0.30	3.3	Theoretical	3.00	Theoretical
% Change	50	10	Experimental	3.3	15
				4.4	16.5
				33	14.7
Duct Tape	0.45	4.4		9.8	17.8
				8.00	
				6.75	

APPENDIX I COMPLETE GANTT CHART



APPENDIX J BRAINSTORMING CONCEPTS

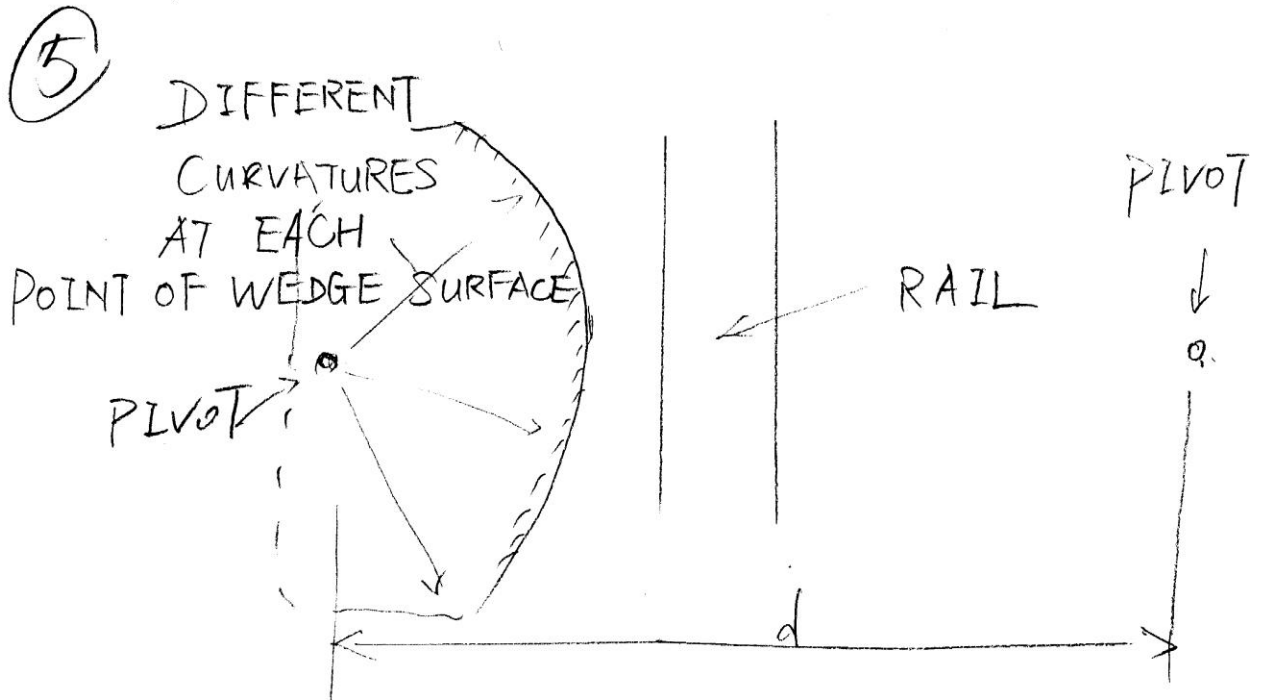
J.1 Adjustable U-Spring



Adjustable U-Spring

Mass-Spring accelerometer senses deceleration and adjusts wheels. Wheels turn screws in the U-spring with opposite threads and either tightens or loosens spring.

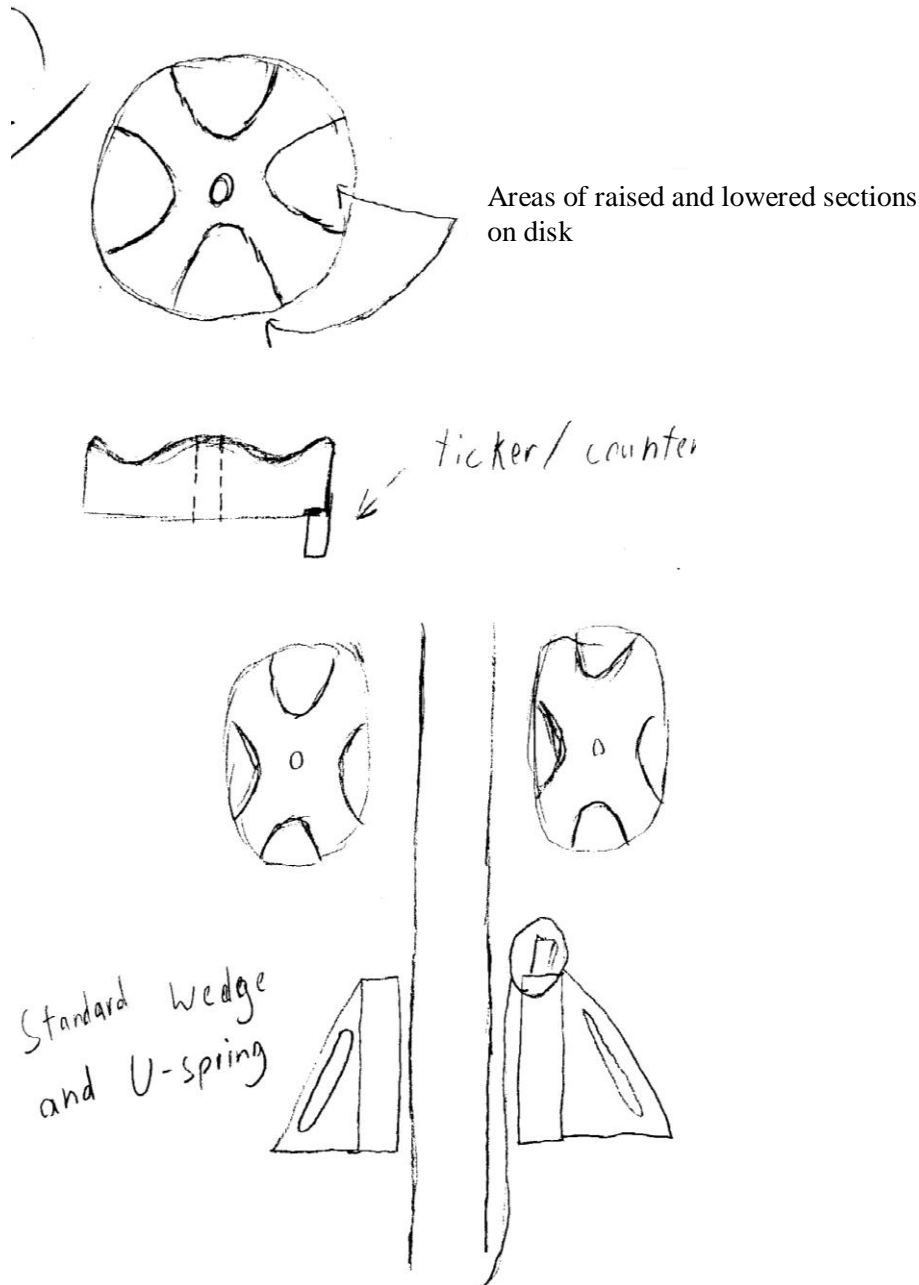
J.2 Wedge of Variable Radius



Wedge of Variable Radius

Idea is that a wedge having varying radii can be rotated to provide increasing or decreasing normal force.

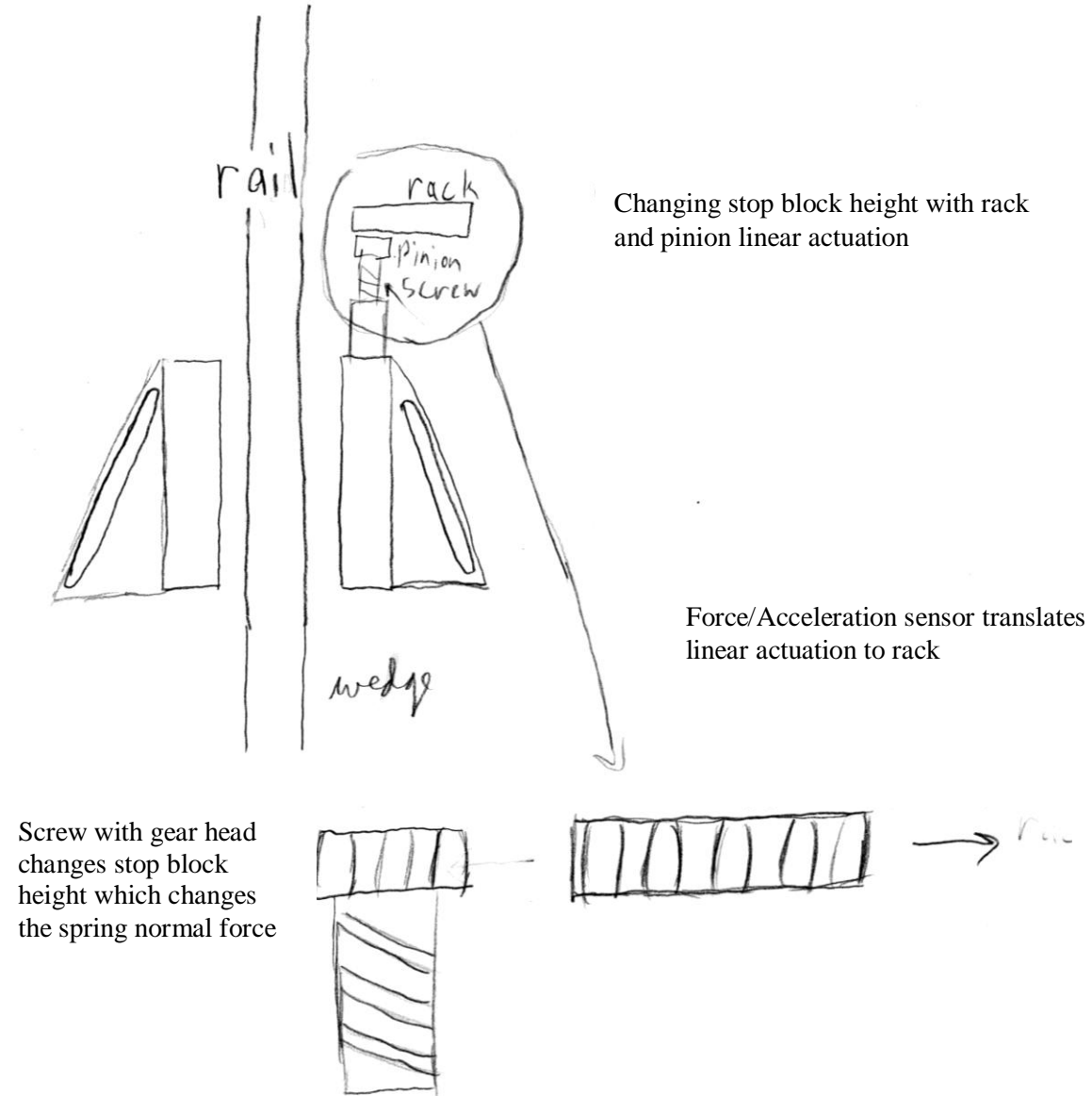
J.3 ABS Braking Concept



ABS Braking Concept

Two disk shaped wedges clamp onto the rail during actuation. The disks have areas of raised and lowered positions that allow the disk to rotate and act similar to an ABS brake. This rotation could be coupled to a ticker/counter that would indicate the speed of the car and could be used to actuate a ratcheting device that changes the normal force.

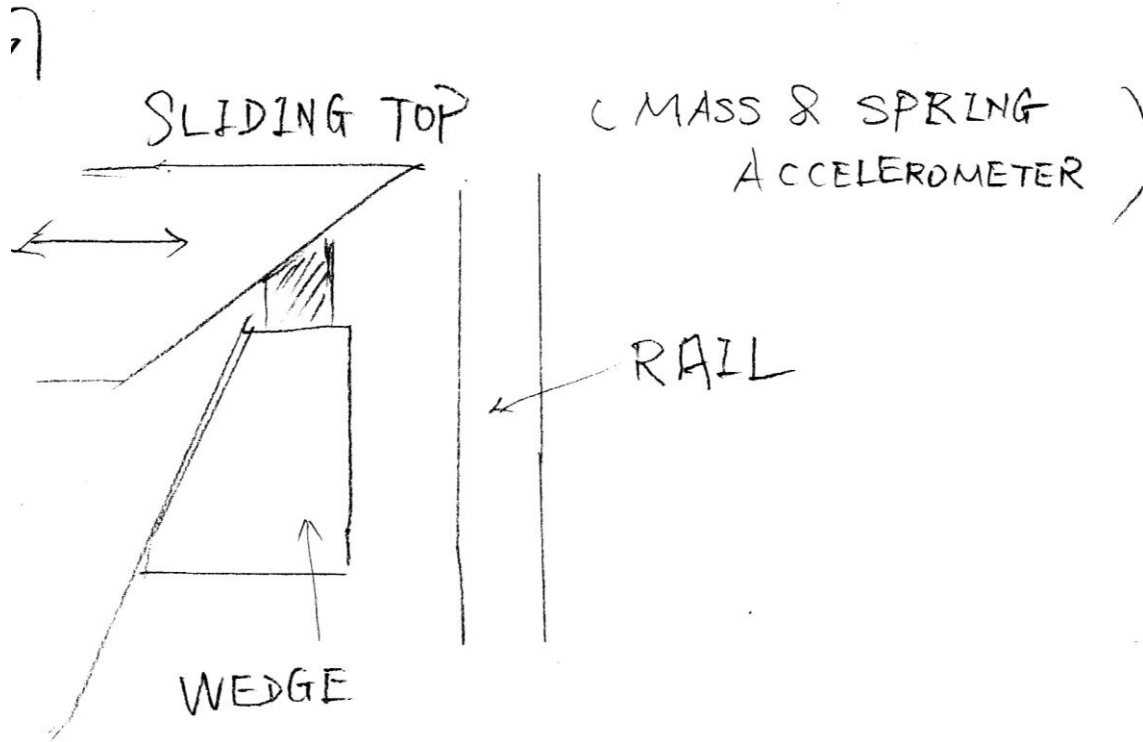
J.4 Screwy Stop Block



Screwy Stop Block

The stop block is attached to a screw that rotates in and out of the wedge to adjust the normal force. Idea is that the friction sensor could translate linear motion into a rack and pinion and the mechanical advantage of the screw would be enough to change the normal force.

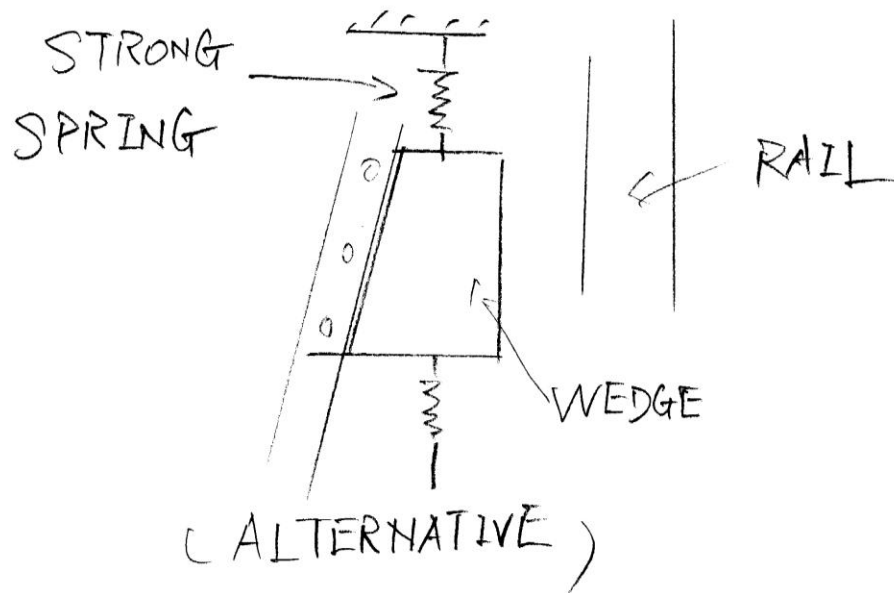
J.5 Adjustable Stop Block



Adjustable Stop Block

Similar concept to the "Screwy Stop block" concept except the stop block is adjusted by a cam system which subsequently adjusts the normal force.

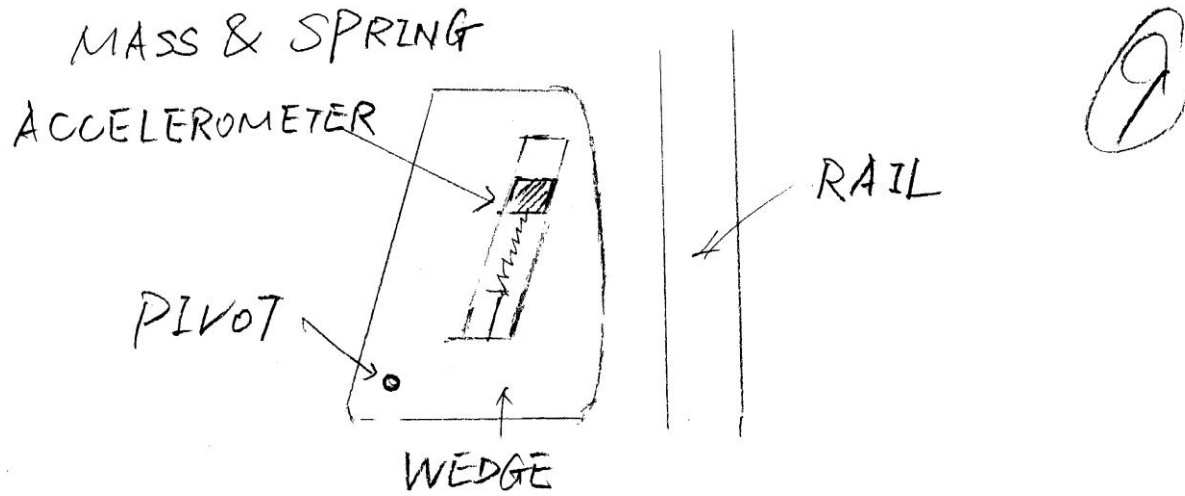
J.6 Spring-Adjusted Stop Block



Spring-Adjusted Stop block

Concept is that a spring replaces the stop block and adjusts the position of the wedge so as to adjust the normal force.

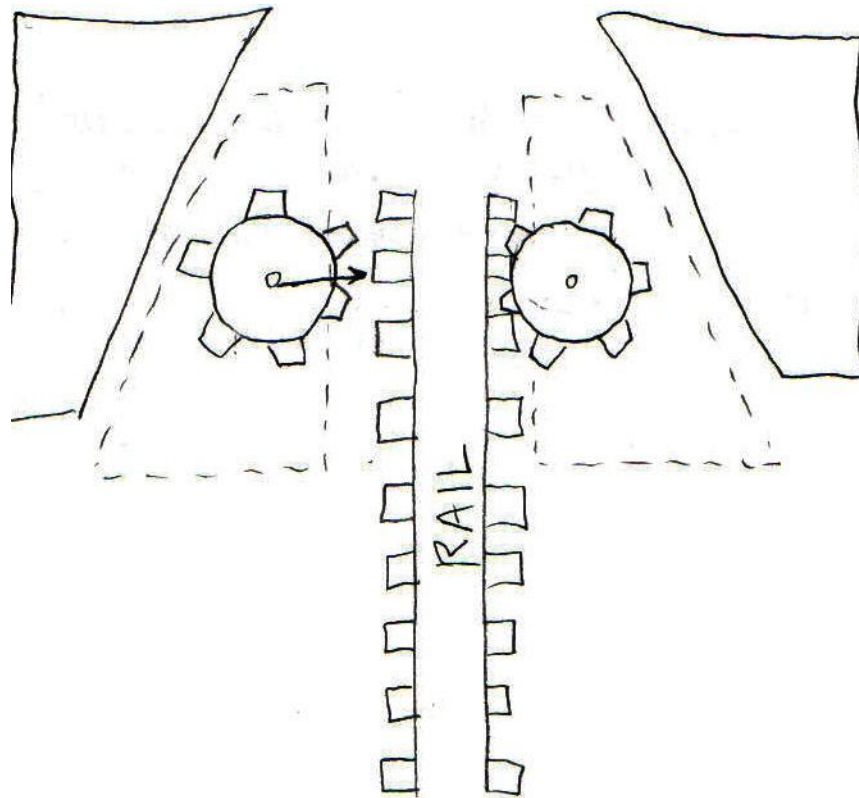
J.7 Mass-Spring Accelerometer Cam



Mass Spring Accelerometer Cam

This design incorporates the mass spring accelerometer into a cam. The idea being that the cam can provide more or less normal force by moving positions in the wedge according to the deceleration. Because the mass is offset from the pivot point, the cam will rotate when the deceleration changes.

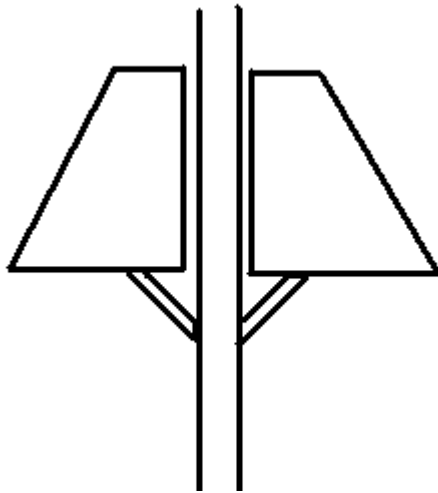
J.8 Toothed Rail & Locking Gears



Toothed Rail & Locking Gears

The guide rail has gear teeth running along its entire length. When the safety engages, gears attached to the wedges engage the rail teeth and disk brakes are used to stop the gears, which in turn stops the car. The stopping does not depend on friction.

J.9 Rail scraper



← Scrapers under the wedges

Scraper

This design aims at scraping the surface of the rail so that the coefficient of friction would be more consistent. The scrapers are under the brake surfaces such that the surface of the rails would be cleaned before the brakes contact those parts of the rail.

APPENDIX K PROTOTYPE PHOTOGRAPHS



Figure 31. Inclined plane friction test



Figure 32. Friction surfaces: duct tape (top), packaging tape (middle), Teflon tape (bottom)

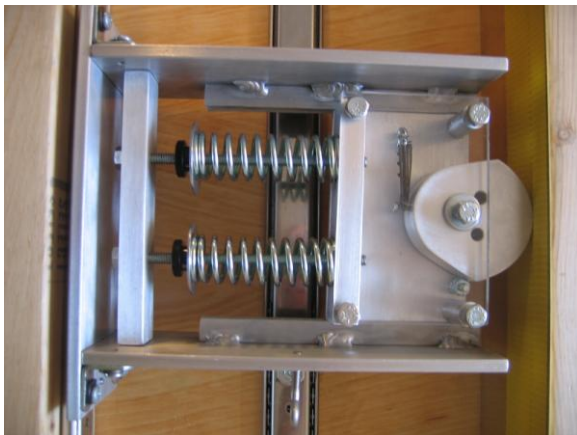


Figure 33. Top view of prototype



Figure 34. Overview of prototype



Figure 35. Prototype shown with cam in un-rotated position

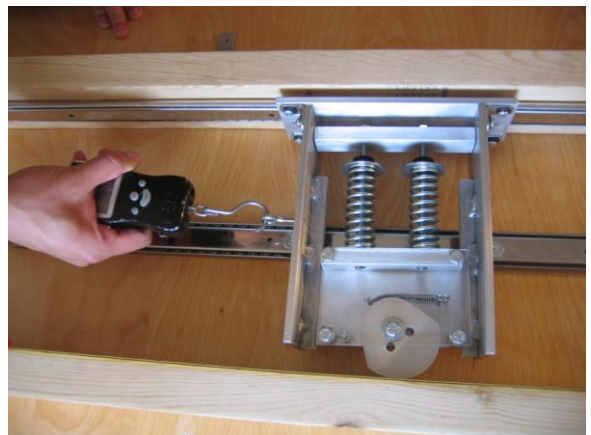


Figure 36. Prototype shown with cam in rotated position

APPENDIX L DESIGN ANALYSES

L.1 Material Selection

Two major parts of the final design are the rotating cam and the brake shoe. The rotating cam is the critical part of the mechanism, as it rotates according to changing friction. The cam is attached to the brake shoe by a set of gear teeth and the brake shoe contacts the rail directly and is essential for stopping the elevator. Both components have similar requirements, including high yield and compressive strength, low density, and high working temperature. A low price is also preferred, as the customer indicated that the budget should be under \$200 for the production of one elevator block. Although not an explicit customer requirement, the system should be as light as possible while being robust. With CES software, constraints were set for determining the appropriate materials.

For the cam, the density and the strength-to-density ratio were crucial, thus they were the axes of the plotted graph. With the price constraint of a maximum \$1/lb, only strong materials with iron as base metal were left to choose from. The top five materials are stainless steel, tool steel, normalized low alloy steel, high silicon cast iron and tempered low alloy steel (see Figure 37). The final selection is low alloy steel, AISI 8650 (tempered @ 425C, oil quenched) because it is the cheapest of the five, and it has a relatively high strength-to-density ratio in the steel group. More information is supplied in Table 8.

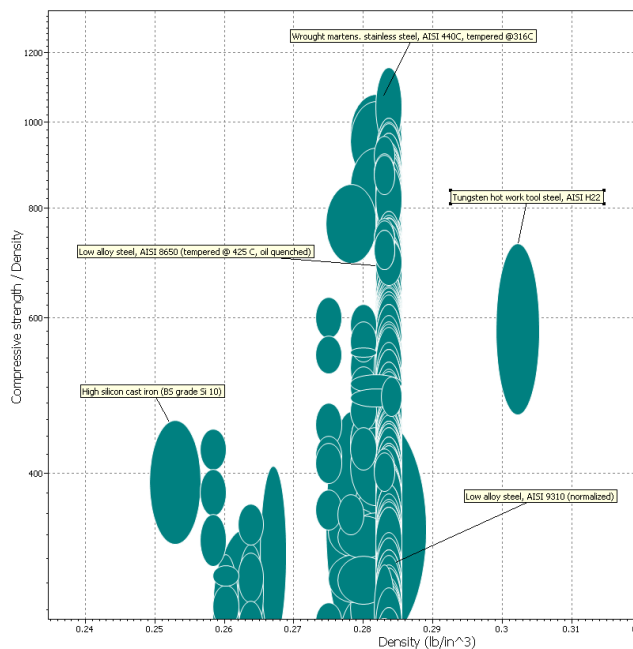


**Figure 37. Cam material options—
low alloy steel is the primary option**

General

Designation

Low alloy steel, AISI 8650 (tempered @ 425 C, oil quenched)

Density	0.2818	-	0.2854	lb/in ³
Price	* 0.3193	-	0.4575	USD/lb

Composition

Composition (summary)

Fe/48-53C/4-6Cr/4-7Ni/75-1Mn/15-.3Si/15-.25Mo/<.035P/<.04S

Base	Fe (Iron)			
C (carbon)	0.48	-	0.53	%
Cr (chromium)	0.4	-	0.6	%
Fe (iron)	96.55	-	97.67	%
Mn (manganese)	0.75	-	1	%
Mo (molybdenum)	0.15	-	0.25	%
Ni (nickel)	0.4	-	0.7	%
P (phosphorus)	0	-	0.035	%
S (sulfur)	0	-	0.04	%
Si (silicon)	0.15	-	0.3	%

Mechanical

Young's modulus	29.88	-	31.33	10 ⁶ psi
Shear modulus	11.46	-	12.33	10 ⁶ psi
Bulk modulus	23.06	-	25.53	10 ⁶ psi
Poisson's ratio	0.285	-	0.295	
Yield strength (elastic limit)	172.6	-	211	ksi
Tensile strength	188.5	-	231.3	ksi
Compressive strength	172.6	-	211	ksi
Flexural strength (modulus of rupture)	172.6	-	211	ksi
Elongation	9	-	15	%
Hardness - Vickers	375	-	465	HV
Fatigue strength at 10 ⁷ cycles	* 74.55	-	86.15	ksi
Fracture toughness	* 29.12	-	51.87	ksi.in ^{1/2}
Mechanical loss coefficient	* 2.7e-4	-	3.4e-4	

Thermal

Melting point	2566	-	2728	°F
Maximum service temperature	* 725	-	779	°F
Minimum service temperature	* -72.4	-	-18.4	°F
Thermal conductivity	* 20.22	-	26	BTU.ft/h.ft ² .F
Specific heat	* 0.1099	-	0.1194	BTU/lb.F
Thermal expansion coefficient	6.111	-	6.944	µstrain/°F

Table 8. Low alloy steel AISI 8650 specifications

For the brake shoe, the requirements are almost identical to those of the cam, thus the procedure for selecting the material is the same as the cam. The top five materials are high silicon cast iron, high Cr white cast iron, carbon steel, stainless steel and Ni-Cr white cast iron. An extra consideration is that cast iron seemed to be a reasonable choice as it is currently used in the elevator safety systems. Thus, the material selected is Ni-Cr white cast iron (BS grade 2B), as it is the cheapest and has a relatively low density among the cast iron choices. More information is supplied in Table 9.

General

Designation

White CI: Ni-Cr, BS grade 2B

Density	0.2746	-	0.2818	lb/in ³
Price	*0.6116	-	0.7183	USD/lb

Composition

Composition (summary)

Fe/3.2-3.6C/3-.8Si/2-.8Mn/3-5.5Ni/1.5-3.5Cr/<.2P/<.5Mo/<.15S

Base	Fe (Iron)			
C (carbon)	3.2	-	3.6	%
Cr (chromium)	1.5	-	3.5	%
Fe (iron)	84.95	-	91.8	%
Mn (manganese)	0.2	-	0.8	%
Mo (molybdenum)	0	-	0.5	%
Ni (nickel)	3	-	5.5	%
P (phosphorus)	0	-	0.2	%
S (sulfur)	0	-	0.15	%
Si (silicon)	0.3	-	0.8	%

Mechanical

Young's modulus	23.93	-	26.11	10 ⁶ psi
Shear modulus	9.282	-	10.3	10 ⁶ psi
Bulk modulus	17.26	-	19.87	10 ⁶ psi
Poisson's ratio	0.27	-	0.28	
Yield strength (elastic limit)	*36.26	-	65.27	ksi
Tensile strength	36.26	-	65.27	ksi
Compressive strength	*72.52	-	130.5	ksi
Flexural strength (modulus of rupture)	69.62	-	123.3	ksi
Elongation	0	-		%
Hardness - Vickers	575	-	635	HV
Fatigue strength at 10 ⁷ cycles	*14.5	-	26.11	ksi
Fracture toughness	*9.1	-	23.66	ksi.in ^{1/2}
Mechanical loss coefficient	*1.5e-3	-	3e-3	

Thermal

Melting point	2066	-	2259	°F
Maximum service temperature	896	-	1004	°F
Minimum service temperature	*5	-	59	°F

Table 9. Ni-Cr white cast iron specifications

L.2 Design for Assembly

A design for assembly analysis was performed for our final design to see if changes could be made to make our design more efficient for assembly. Our final design incorporates several elements of current elevator safety technology, thus our analysis focuses on the main area of deviation: the cam frame sub-assembly. Specifically, the analysis is of the 9 elements that make up the cam frame assembly (see Figure 38). These elements were analyzed using manual handling and insertion DFA charts and it was found that assembly should take 62.44 seconds and have an efficiency of 0.37 (see Table 10, p. 59). The design was tested for the minimum number of parts and it was found that three parts (6, 7, 8) can be combined into one piece. The new analysis shows that the assembly will take 42.54 seconds and have an efficiency of 0.49.

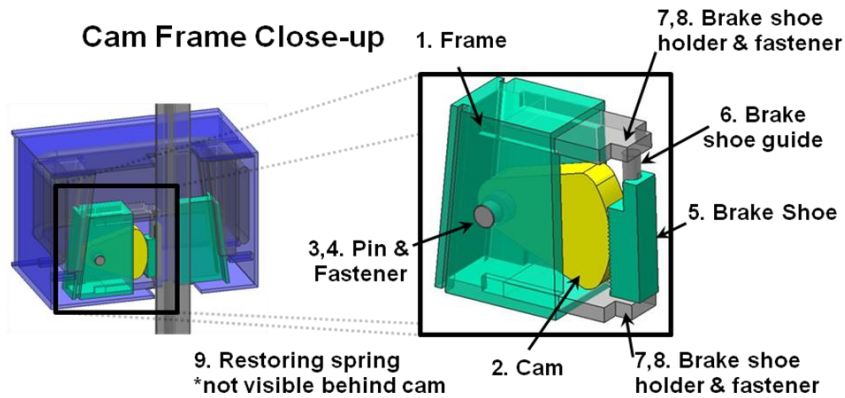


Figure 38. Final design cam frame sub-assembly

Original Design

Part ID #	Number of times the operation is carried out consecutively	two- digit manual handling code	manual handling time per part	two-digit manual insertion code	manual insertion time per part	operation time (sec) [2]*[4]+[6]	operation costs (cents) [.4]*[7]	figures for estimates of theoretical minimum parts	Part
1	1	30	1.95	0	1.5	3.45	1.38	1	Frame
2	1	20	1.8	30	2	3.8	1.52	1	Cam
3	1	10	1.5	41	7.5	9	3.6	1	Pin
4	1	10	1.5	32	4	5.5	2.2	1	Pin fastener (cotter pin)
5	1	30	1.95	30	2	3.95	1.58	1	Brake shoe
6	1	10	1.5	50	6	7.5	3	1	Brake shoe guide
7	2	10	1.95	31	5	8.9	3.56	0	Brake guide holder
8	2	30	1.5	39	8	11	4.4	0	Brake guide fastener
9	1	15	1.84	43	7.5	9.34	3.736	1	Restoring Spring

Tm: Cm: Nm:
62.44 24.976 7

Efficiency 0.336323

Improved Design

Part ID #	Number of times the operation is carried out consecutively	two- digit manual handling code	manual handling time per part	two-digit manual insertion code	manual insertion time per part	operation time (sec) [2]*[4]+[6]	operation costs (cents) [.4]*[7]	figures for estimates of theoretical minimum parts	Part
1	1	30	1.95	0	1.5	3.45	1.38	1	Frame
2	1	20	1.8	30	2	3.8	1.52	1	Cam
3	1	10	1.5	41	7.5	9	3.6	1	Pin
4	1	10	1.5	32	4	5.5	2.2	1	Pin fastener (cotter pin)
5	1	30	1.95	30	2	3.95	1.58	1	Brake shoe
6	1	10	1.5	50	6	7.5	3	1	Brake shoe guide assembly
9	1	15	1.84	43	7.5	9.34	3.736	1	Restoring Spring

Tm: Cm: Nm:
42.54 17.016 7

Efficiency 0.493653

Table 10. DFA Chart for cam frame sub-assembly

L.3 Design for Environmental Sustainability

Using SimaPro, a design for environment analysis was performed for the cast iron of the brake shoe (weighing 3.1 kg) and the high strength steel of the cam (weighing 12.2kg). The total mass of air emissions, water emissions, use of raw materials and solid waste can be seen in Figure 39.

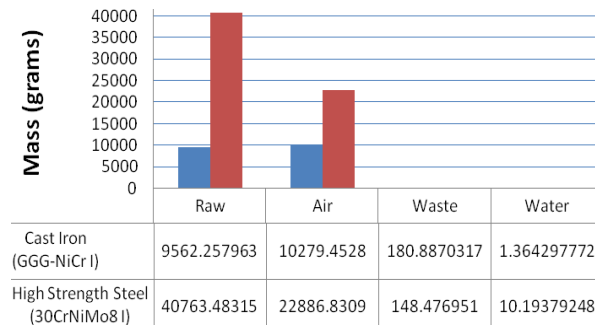


Figure 39. Total material/emissions for cam & brake shoe

Using the EcoIndicator 99 damage classifications (see Figure 40 and Figure 41), it was found that the high strength steel had the highest classification in each of the areas of human health, ecosystem quality, and resources with a total point score of 13.5 pts (see Figure 42, p. 61). The cast iron closely follows the steel with a total point score of 11.8. Based on the EcoIndicator point value it is apparent that the resources category is most important with almost 90% of the total points. When the two materials are compared for a life cycle assessment it is difficult to determine which has a bigger impact because they are very similar materials but it appears that the high strength steel will have a slightly larger impact.

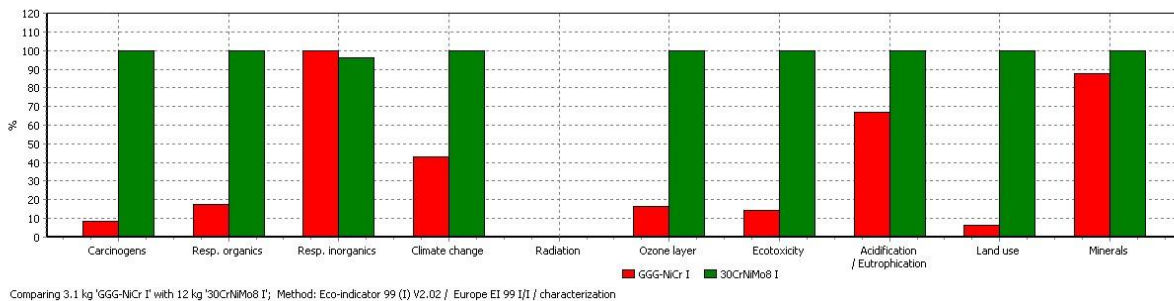


Figure 40. Relative impacts of brake shoe (red) and cam (green) for EcoIndicator 99 disaggregated damage classifications

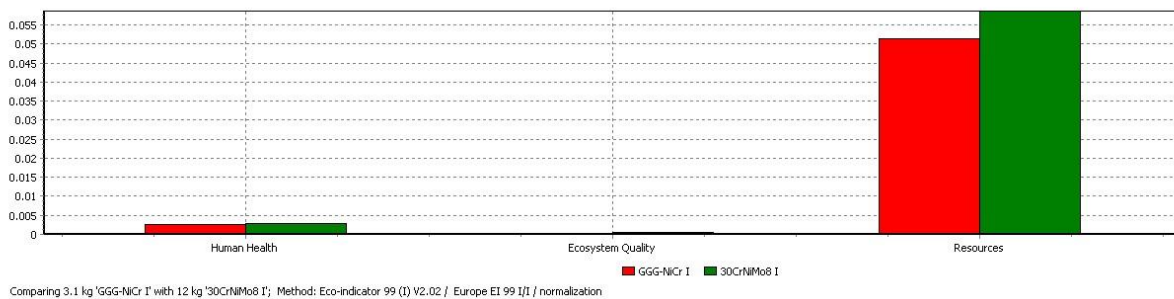


Figure 41. Normalized scores of brake shoe (red) and cam (green) for EcoIndicator 99 damage meta-categories

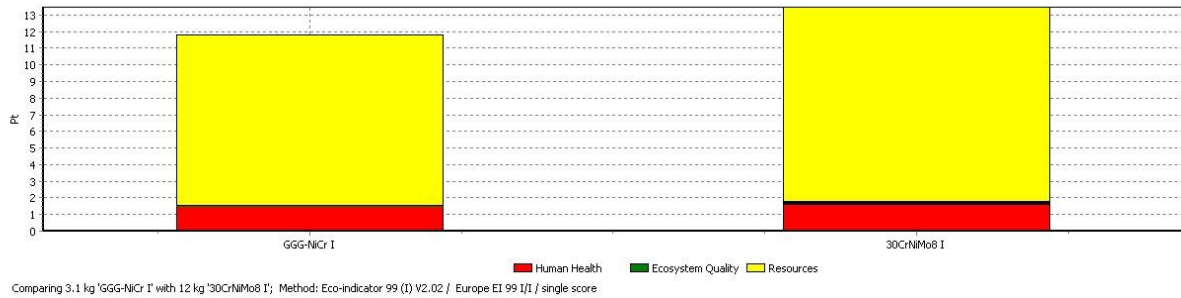


Figure 42. Ecolndicator total point values for brake shoe (left) and cam (right)

L.4 Design for Safety

The major risks for the prototype relate to machining and assembly. The fabrication phase requires the use of a mill, band saw, drill press, and arbor press—all of which can be dangerous to the user if operated improperly. Beyond fabrication, the prototype does not pose major safety concerns to the user because the spring forces involved are small. At the worst, a person’s finger could become pinched in the cam mechanism. In addition, the risk of losing or damaging parts during transportation or testing would cause the system to be non-functional.

For the final design, the major risk would be the failure of springs or the cam due to high stresses or heat. If such failure occurs, any passengers in the elevator car may be injured due to the malfunction of the braking system. From the DesignSafe analysis (see Table 11), there are not many risks regarding the system, due to the fact that it is purely mechanical and users do not interact with it directly or regularly. The main risk is the failure of system due to stress and heat, which is addressed by the rack-and-pinion mechanism.

Controlled Elevator Safety Mechanism

4/14/2008

designsafe Report

Application: Controlled Elevator Safety Mechanism Analyst Name(s):
 Description: Company:
 Product Identifier: Facility Location:
 Assessment Type: Detailed
 Limits:
 Sources:
 Guide sentence: When doing [task], the [user] could be injured by the [hazard] due to the [failure mode].

User / Task	Hazard / Failure Mode	Initial Assessment		Risk Reduction Methods /Comments	Final Assessment		Status / Responsible /Reference
		Severity Exposure Probability	Risk Level		Severity Exposure Probability	Risk Level	
All Users All Tasks	mechanical : unexpected start Unexpected actuation during normal operation of elevator	Slight None Negligible	Low	Check cable connections periodically			
All Users All Tasks	mechanical : break up during operation Cam endures high stress	Catastrophic Remote Possible	High	Calculate stress applied for different elevator systems			

Table 11. DesignSafe risk analysis

Risk assessment is the general consideration for risks of the design in the technical sense, and FMEA considers every possible failure modes that a system may encounter and also provide possible solutions to fix it. The difference between acceptable risk and zero risk is the probability of the risk to occur. Zero risk is difficult to achieve, and it may be too costly an approach for any systems. With a large factor of safety, acceptable risk may be achieved and thus the product is considered as safe. This distinction shows up in our project, as there are materials which could be safer in terms of operational parameters, but they are too expensive to be used, thus we used other materials which are acceptably safe instead.

L.5 Manufacturing Process Selection

Our sponsor, Otis, gave us a target production volume of 40,000 elevator safety blocks are needed to be produced annually (20,000 elevators \times 2 safety blocks/elevator). To mass produce the safety systems, the manufacturing processes should be as cheap and efficient as possible. The rack-and-pinion subsystem comprises a rotating cam and a brake shoe which are connected by a set of gear teeth.

The cam is made of low alloy steel, and its geometry should be created from a die cast. A hole is needed for the pin and this hole requires tighter tolerances, thus it should be drilled and reamed. Because casting the gear teeth will likely not meet the required tolerances, it will be necessary to mill the teeth. The surface should be mechanically polished to remove surface imperfections.

The brake shoe is made of cast iron, which cannot be die casted, so its shape can be investment casted instead. Again, milling is necessary for the exact dimensions of the teeth and polishing is required to create surfaces desired for braking. These processes are confirmed with CES manufacturing process selector (see Figure 43). The main cost here is for the casts, but the die cast could be used repeatedly and investment casts can create a large batch of brake shoes at the same time, thus they are economical for the large production volume.



Figure 43. CES Manufacturing Process Selector recommendations for Cam (left) and Brake Shoe (right)